A clathrin-dependent pathway leads to KRas signaling on late endosomes en route to lysosomes

Albert Lu,[1] Francesc Tebar,[1] Blanca Alvarez-Moya,[1] Cristina López-Alcalá,[1] Maria Calvo,[2] Carlos Enrich,[1] Neus Agell,[1] Takeshi Nakamura,[3] Michiyuki Matsuda,[3] and Oriol Bachs[1]

[1]Departament de Biologia Cellular, Immunologia i Neurociències, Institut d'Investigacions Biomèdiques August Pi i Sunyer and [2]Unitat de Microscòpia Confocal, Serveis Cientificotècnics, Facultat de Medicina, Universitat de Barcelona, 08036 Barcelona, Spain
[3]Department of Pathology and Biology of Diseases, Graduate School of Medicine, Kyoto University, Sakyo-ku, Kyoto 606-8501, Japan

Ras proteins are small guanosine triphosphatases involved in the regulation of important cellular functions such as proliferation, differentiation, and apoptosis. Understanding the intracellular trafficking of Ras proteins is crucial to identify novel Ras signaling platforms. In this study, we report that epidermal growth factor triggers Kirsten Ras (KRas) translocation onto endosomal membranes (independently of calmodulin and protein kinase C phosphorylation) through a clathrin-dependent pathway. From early endosomes, KRas but not Harvey Ras or neuroblastoma Ras is sorted and transported to late endosomes (LEs) and lysosomes. Using yellow fluorescent protein–Raf1 and the Raichu-KRas probe, we identified for the first time in vivo–active KRas on Rab7 LEs, eliciting a signal output through Raf1. On these LEs, we also identified the p14–MP1 scaffolding complex and activated extracellular signal-regulated kinase 1/2. Abrogation of lysosomal function leads to a sustained late endosomal mitogen-activated protein kinase signal output. Altogether, this study reveals novel aspects about KRas intracellular trafficking and signaling, shedding new light on the mechanisms controlling Ras regulation in the cell.

Introduction

Ras proteins are small GTPases involved in the regulation of important cellular functions such as proliferation, differentiation, and apoptosis (Malumbres and Barbacid, 2003). The activity of Ras depends on its association with guanine nucleotides, being inactive when bound to GDP and active when associated with GTP. Ras proteins have an intrinsic low GTPase activity that is increased by GTPase-activating proteins. The activity of Ras is regulated by extracellular factors that activate receptor Tyr kinases and recruit guanine nucleotide exchange factors to the plasma membrane (PM), promoting the Ras-GDP to Ras-GTP conversion, which induces a conformational change that allows association of Ras with effectors, including Raf1, PI3K, or Ral–guanine nucleotide dissociation stimulator, that become activated.

At the PM, Ras isoforms have distinct locations, which depend on their guanine nucleotide status. Thus, in the GDP conformation, Harvey Ras (HRas) resides in cholesterol-rich domains (Roy et al., 1999; Prior et al., 2001), whereas upon GTP loading, it is recruited to cholesterol-poor domains. In contrast, GDP–neuroblastoma Ras (NRas) is resident in cholesterol-poor domains and moves to cholesterol-rich domains when loaded with GTP. Finally, Kirsten Ras (KRas)–GDP normally resides in cholesterol-poor domains, and no clear lateral segregation has been reported to occur after GTP loading. It is becoming evident that the differential Ras partitioning and nanoclustering within the PM influence the generation and transmission of distinct signal outputs (Hancock, 2003; Tian et al., 2007).

The presence of HRas and NRas in the Golgi complex is not transient, and it has been shown that these isoforms are active on this compartment (Chiu et al., 2002; Bivona et al., 2003; Caloca et al., 2003; Perez de Castro et al., 2004; Quatela and Philips, 2006). In the majority of cell types, activation of Ras isoforms at the PM is fast and transient, whereas its activation at the Golgi is delayed and more sustained (Chiu et al., 2002). However, it has been shown that stimulation of primary or Jurkat

Correspondence to Oriol Bachs: obachs@ub.edu

Abbreviations used in this paper: BIM, bisindolylmaleimide; CHX, cycloheximide; EE, early endosome; EGFR, EGF receptor; ERK, extracellular signal-regulated kinase; FRET, fluorescence recovery energy transfer; HRas, Harvey Ras; KRas, Kirsten Ras; LBPA, lysobisphosphatidic acid; LE, late endosome; MEK, MAPK/ERK kinase; mRFP, monomeric RFP; MVB, multivesicular body; NRas, neuroblastoma Ras; pERK, phospho-ERK; PM, plasma membrane.

The Rockefeller University Press $30.00
J. Cell Biol. Vol. 184 No. 6 863–879
www.jcb.org/cgi/doi/10.1083/jcb.200807186

T cells induced Ras activation exclusively on the Golgi, and there, activation is dependent on Ca^{2+}, phospholipase Cγ, and the guanine nucleotide exchange factor RasGPR1 (Bivona et al., 2003; Caloca et al., 2003; Perez de Castro et al., 2004). HRas targeted to the Golgi apparatus or to the ER retained its full transforming activity, indicating that the signaling required for transformation can also be initiated from internal membranes. However, the signaling pathways activated in each case are slightly different (Chiu et al., 2002). Thus, Ras signal outputs are determined to some extent by the intracellular location from which signaling arises.

It has been shown that Ras can activate endocytosis by directly regulating the Rab5 nucleotide exchange activity of RIN1 (Tall et al., 2001). Ras has also been found in the endocytic compartment (Pol et al., 1998; Howe et al., 2001; Jiang and Sorkin, 2002; Roy et al., 2002; Fivaz and Meyer, 2005; Gomez and Daniotti, 2005; Jura et al., 2006).

The transit of Ras from PMs to endosomes has been well documented for the HRas isoform (Jiang and Sorkin, 2002; Roy et al., 2002; Gomez and Daniotti, 2005; Jura et al., 2006); HRas colocalizes with EGF receptor (EGFR) on early endosomes (EEs), where it engages Raf1 and triggers signaling activity. It has also been reported that endocytosis is required for maximal HRas signal output (Roy et al., 2002). In contrast, KRas is less retained on endosomes, probably as a result of a faster recycling to the PM (Jiang and Sorkin, 2002; Roy et al., 2002). HRas and NRas can be ubiquitylated, which stabilizes their interaction with endosomal membranes. KRas is refractory to ubiquitylation (Jura et al., 2006).

KRas specifically interacts with CaM (Villalonga et al., 2001). In rat hippocampal neurons stimulated by glutamate, KRas recruits Ca^{2+}/CaM to the PM, inducing its translocation to Golgi and endosomal membranes (Fivaz and Meyer, 2005). Interestingly, KRas can also be translocated from the PM to the ER, Golgi apparatus, and the outer mitochondrial membrane (Bivona et al., 2006) by a PKC-mediated phosphorylation mechanism. On mitochondria, KRas associates with Bcl-Xl and induces apoptosis.

Several crucial aspects of the intracellular trafficking and signaling of KRas remain unclear. In this study, we have analyzed in detail and for the first time in vivo the trafficking of KRas from the PM along the endosomal compartment. The results reported in this study reveal that KRas is internalized through a clathrin-dependent mechanism and is transported along EEs, late endosomes (LEs), and eventually into lysosomes. KRas is active on the LE and together with the p14–MP1 scaffolding complex constitutes an intracellular signaling platform.

Results

Localization of KRas on the early endosomal compartment

GFP-KRas was transiently transfected in COS-1 cells, and its presence on endosomes was analyzed by confocal microscopy. For all purposes, we chose only cells with similar moderate levels of KRas expression. Fig. 1 A shows that GFP-KRas colocalized with the early endosomal marker EEA1 in starved cells. Colocalization between both molecules was significantly increased when cells were treated with EGF-TRITC for 20 min (Fig. 1, B and C). Image magnification shows clear-cut colocalization in both individual and clustered endosomes (Fig. 1 D).

In vivo, time-lapse video confocal microscopy revealed colocalization of EGF-TRITC with GFP-KRas on EEs at different times after EGF stimulation (Video 1). Moreover, immunocytochemical results also revealed colocalization among GFP-KRas, EGF-TRITC, and the endogenous EGFR (Fig. 1 E). Consistently, this was also confirmed in NIH3T3 cells (clone Wt8) stably expressing EGFR (Fig. 1 F and Fig. S1, A and B). In NIH3T3-Wt8 cells treated with EGF, we also detected a significant increase of GFP-KRas and endogenous KRas together with the EGFR in the endosomal fractions isolated by sucrose gradients (Fig. 1, G and H, respectively). Endosomal fractions were prepared as described previously (Grewal et al., 2000). Colocalization of endocytosed rhodamine-labeled transferrin with GFP-KRas on EEs was also observed (Fig. S1 C). These results indicate that a certain fraction of KRas localizes on EEs after EGF stimulation.

Endosomal translocation of KRas is independent of CaM and PKC phosphorylation

A recent study argued for a relevant role of CaM in the translocation of PM-bound KRas to Golgi and endosomal membranes of hippocampal neurons stimulated by glutamate (Fivaz and Meyer, 2005). Thus, we aimed to analyze the role of CaM in the regulation of KRas translocation to endosomes in COS-1 cells. We first determined the presence of GFP-KRas on EEs in cells pretreated with the CaM antagonist, W13, for 1 h and subsequently stimulated with EGF (Fig. 2 A). Under CaM-inhibitory conditions, we observed clear colocalization of KRas, EGF-TRITC, and EEA1, suggesting that KRas localization on EEs was a CaM-independent process in this cellular type.

It has been reported that PKC phosphorylation on Ser181 of KRas regulates its translocation to intracellular membranes (Bivona et al., 2006; Plowman et al., 2008). To study the effect of PKC phosphorylation on KRas translocation to endosomes, cells were treated with the general PKC inhibitor bisindolylmaleimide (BIM), and the presence of KRas on endosomes was analyzed. Results revealed a clear colocalization among KRas, EEA1, and EGF on intracellular vesicles, indicating that the translocation of KRas to EEs is a PKC-independent process (Fig. 2 B). The endosomal distribution of the pseudophosphorylated mutant YFP-KRas Ser181D or the nonphosphorylatable mutant YFP-KRas Ser181A after EGF treatment confirmed that translocation is independent of Ser181 phosphorylation (Fig. 2, C and D). Although the KRas Ser181D mutant does not bind CaM, KRas Ser181A still retains this ability (Lopez-Alcala et al., 2008). We observed that KRas Ser181A translocates to endosomes in the presence of W13 (Fig. 2 E), confirming that KRas translocation to endosomes is CaM independent. Interestingly, EGF stimulation increases the relative colocalization of KRas (wild-type and Ser181 mutants) with EEA1 in all of the aforementioned conditions (see quantifications in Fig. 2).

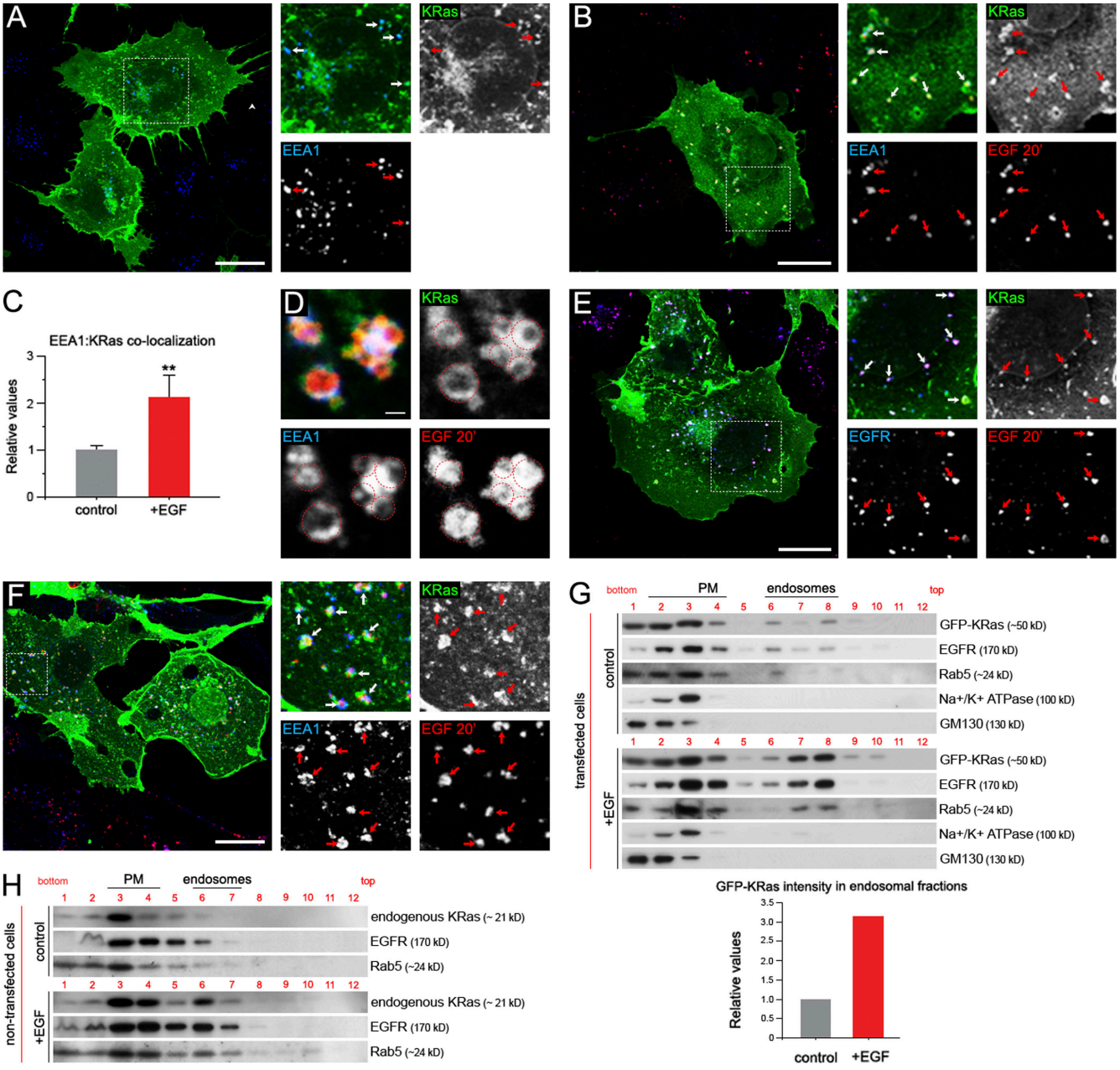

Figure 1. **EGF induces KRas translocation to the early endosomal compartment.** COS-1 cells were transiently transfected with GFP-KRas, and its intracellular localization was analyzed by confocal microscopy. (A) Colocalization of GFP-KRas and EEA1 on intracellular structures. (B) Cells treated with 100 ng/ml EGF-TRITC for 20 min show increased colocalization between GFP-KRas, EEA1, and EGF-TRITC. (C) Quantification of cells in B. Statistical significances of differences between control and EGF treatment were determined using the Student's *t* test. Data are means ± SEM; **, $P < 0.01$. (D) A more detailed confocal image of early endosomal structures positive for GFP-KRas, EEA1, and EGF-TRITC is shown. Red dotted circles indicate the perimeter of magnified endosomes. (E) Likewise, in EGF-stimulated cells, endocytosed EGFR detected by immunofluorescence colocalizes with GFP-KRas and EGF-TRITC. (F) NIH3T3-Wt8 cells treated with 100 ng/ml EGF-TRITC for 20 min also confirmed colocalization of GFP-KRas, EEA1, and EGF-TRITC. (G) In NIH3T3 cells, a significant increase of GFP-KRas together with EGFR is detected in endosomal fractions isolated by sucrose density gradients after EGF treatment (Western blot), and the results presented are representative of three independent experiments (graph). (H) Similarly, after EGF stimulation, subcellular fractionation by sucrose gradients using nontransfected NIH3T3-Wt8 cells shows enrichment of endogenous KRas and EGFR in endosome fractions (Western blot). Colocalization is indicated with white (merge) or red (separate channels) arrows. (A, B, E, and F) Dotted boxes define the areas from which the corresponding insets were generated. Bars: (A, B, E, and F) 20 µm; (D) 500 nm.

KRas follows the clathrin-dependent endocytic pathway upon EGF stimulation

Next, we focused on the mechanisms by which KRas is endocytosed. Therefore, we examined whether the clathrin-dependent endocytic system could be involved in KRas endosomal translocation. Fig. 3 A shows the presence of GFP-KRas in clathrin-coated pits in starved cells. When cells were incubated with EGF-TRITC, the colocalization was increased (Fig. 3 C). Fig. 3 E shows that GFP-KRas colocalized with EGFR after 2.5 min of EGF-TRITC stimulation.

Incubation of EGF for 1 h at 4°C allows binding of the ligand to its receptor clustered in coated pits, but internalization

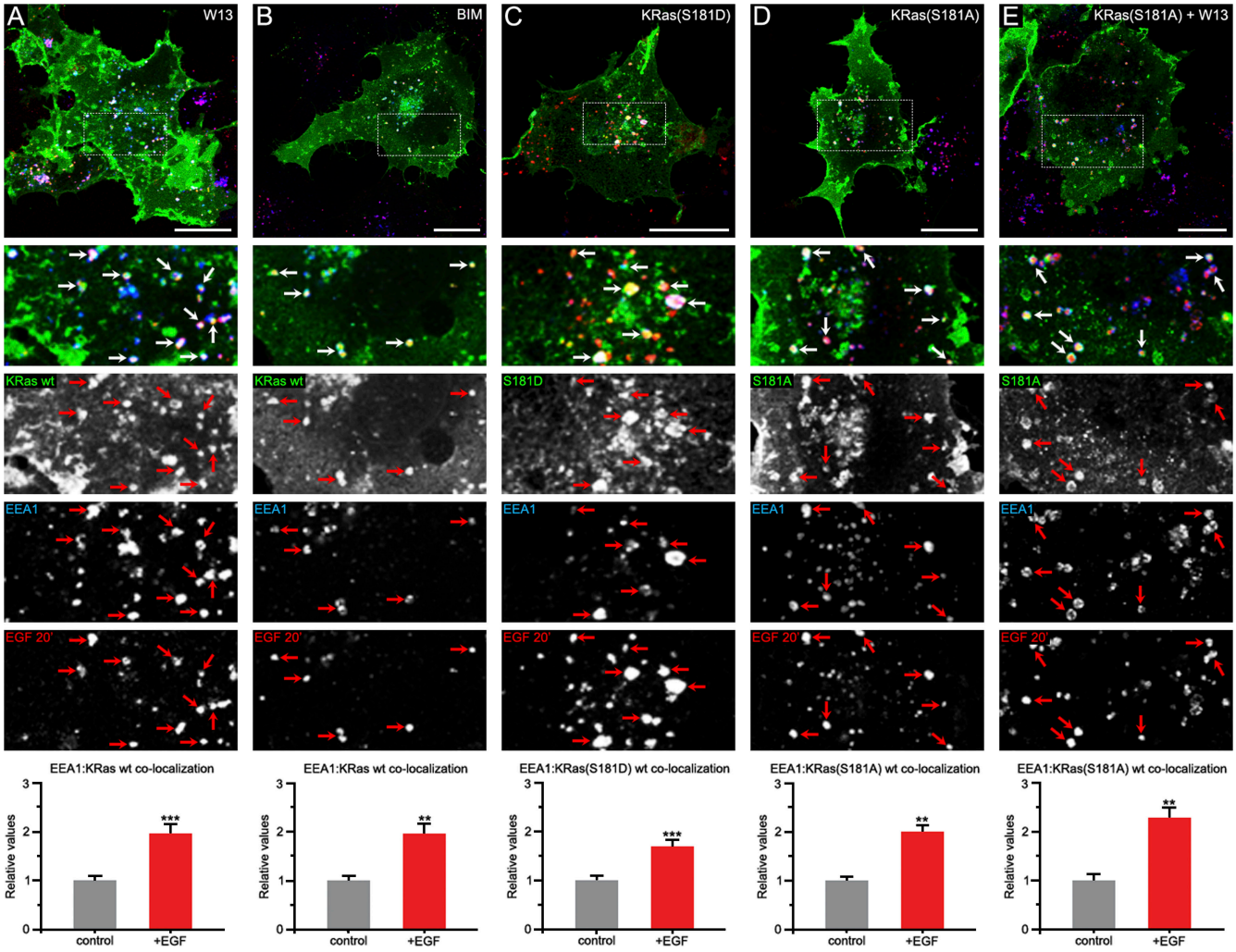

Figure 2. **Translocation of KRas to the early endosomal compartment is a CaM- and PKC-independent process.** COS-1 cells expressing GFP-KRas or the indicated mutants were treated with EGF-TRITC for 20 min, fixed, and immunolabeled with anti-EEA1. (A) Colocalization of GFP-KRas (wild type [wt]), EEA1, and EGF-TRITC on intracellular vesicles was observed after treatment with 10 µg/ml of the CaM inhibitor W13 for 1 h. (B) The same as in A but using 10 µM of the general PKC inhibitor BIM for 1 h. (C) YFP-KRas (Ser181D [S181D]) colocalizes with EEA1 and EGF-TRITC. (D) Similarly, YFP-KRas (Ser181A [S181A]) colocalizes with EEA1 and EGF-TRITC. (E) The presence of YFP-KRas (Ser181A) on EEs was analyzed in cells treated with W13. Quantification of colocalization is shown underneath each panel. Statistical significances of differences between control and EGF treatment were determined using the Student's *t* test. Data are means ± SEM; **, $P < 0.01$; ***, $P < 0.001$. Colocalization is indicated with white (merge) or red (separate channels) arrows. Dotted boxes define the areas from which the corresponding insets were generated. Bars, 20 µm.

remains blocked (Jiang et al., 2003). Thus, after 1 h at 4°C, clathrin detection was performed on starved COS-1 cells expressing GFP-KRas (Fig. 3 B) or on EGF-TRITC–stimulated cells (Fig. 3 D). Results showed some colocalization of clathrin with KRas in nonstimulated cells and an enhanced colocalization of clathrin with KRas and EGF in small punctate structures, corresponding to coated pits.

The possibility that a clathrin-dependent mechanism could participate in the KRas endosomal translocation was investigated in cells transfected with a dynamin-1 mutant (DynK44A) that blocks clathrin- and caveolae-mediated endocytosis (Damke et al., 1994; Oh et al., 1998). In cells expressing this mutant, EGF endocytosis was greatly reduced (Fig. 3 F), and the colocalization of KRas and EEA1 was significantly diminished (Fig. 3 G). These results together with the clear colocalization of KRas and clathrin revealed that KRas internalization is mainly mediated through a clathrin-dependent mechanism.

Enhanced localization of KRas on late endosomal membranes: effects of bafilomycin and U18666A

Because a certain pool of internalized EGFR is sorted from the EE to the late endocytic compartment preceding lysosomal degradation, we aimed to test whether KRas could also follow this late endocytic route. Fig. 4 A confirmed the colocalization between EEA1 and KRas and shows a small fraction of KRas on Rab7-positive LEs.

To improve the detection of KRas on the late endocytic compartment, cells were treated with U18666A, a molecule that inhibits cholesterol transport and alters the trafficking of multivesicular body (MVB)–associated membrane proteins (Liscum and Faust, 1989; de Diego et al., 2002), or with bafilomycin-A1 (B-A1), an inhibitor of vacuolar-type H^+-ATPase that blocks acidification and protein degradation in lysosomes (van Weert et al., 1995; Recchi and Chavrier, 2006). In COS-1 cells, both

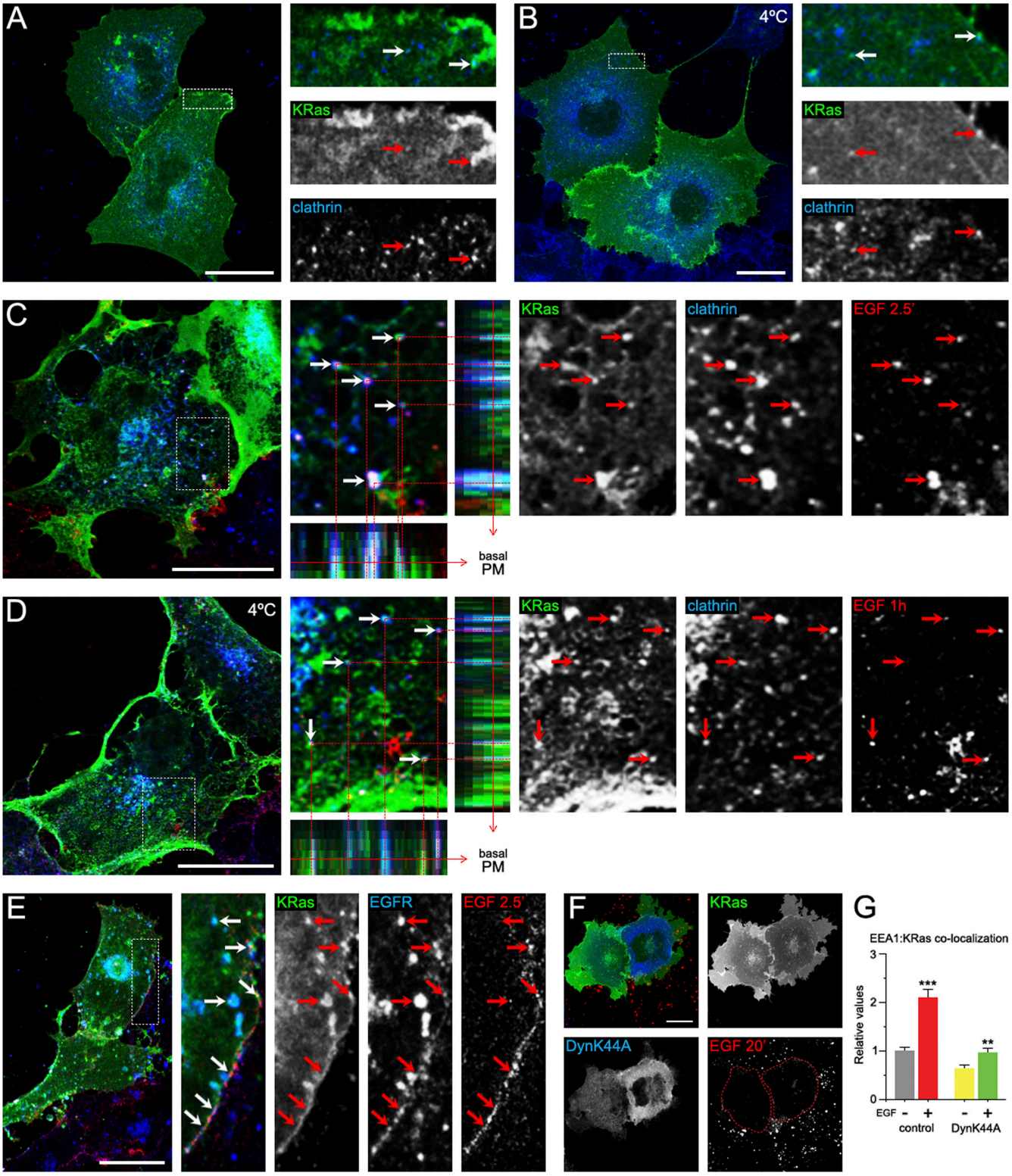

Figure 3. **KRas follows the clathrin-dependent endocytic pathway upon EGF stimulation.** (A–G) COS-1 cells were transiently transfected with GFP-KRas, and its intracellular localization was analyzed by confocal microscopy. (A) Starved cells were fixed and immunolabeled with an anticlathrin antibody. (B) Clathrin detection on starved cells after 1 h at 4°C. (C) Cells treated with EGF-TRITC for 2.5 min were fixed and immunolabeled with an anticlathrin antibody. The red dotted lines point to colocalization in the image and in the z-axis profile. (D) The same as in C, but cells were incubated with EGF-TRITC for 1 h at 4°C. Reconstruction of the z-axis profile was performed to confirm the visualization on basal PM (C and D, insets). (E) Cells treated with EGF-TRITC for 2.5 min were fixed and immunolabeled with anti-EGFR. (F) Cells coexpressing GFP-KRas and the HA-tagged dynamin mutant K44A (DynK44A) were treated with EGF-TRITC for 20 min and immunolabeled with anti-HA. Red dotted contours indicate the perimeter of cells cotransfected with GFP-KRas and HA-DynK44A. (G) Quantification of EEA1 and GFP-KRas colocalization in control and dynamin K44A–expressing cells ± EGF is shown. Statistical significances of differences between control and EGF treatment were determined using the Student's *t* test. Data are means ± SEM; **, $P < 0.01$; ***, $P < 0.001$. (A–E) Colocalization is indicated with white (merge) or red (separate channels) arrows. Dotted boxes define the areas from which the corresponding insets were generated. Bars, 20 µm.

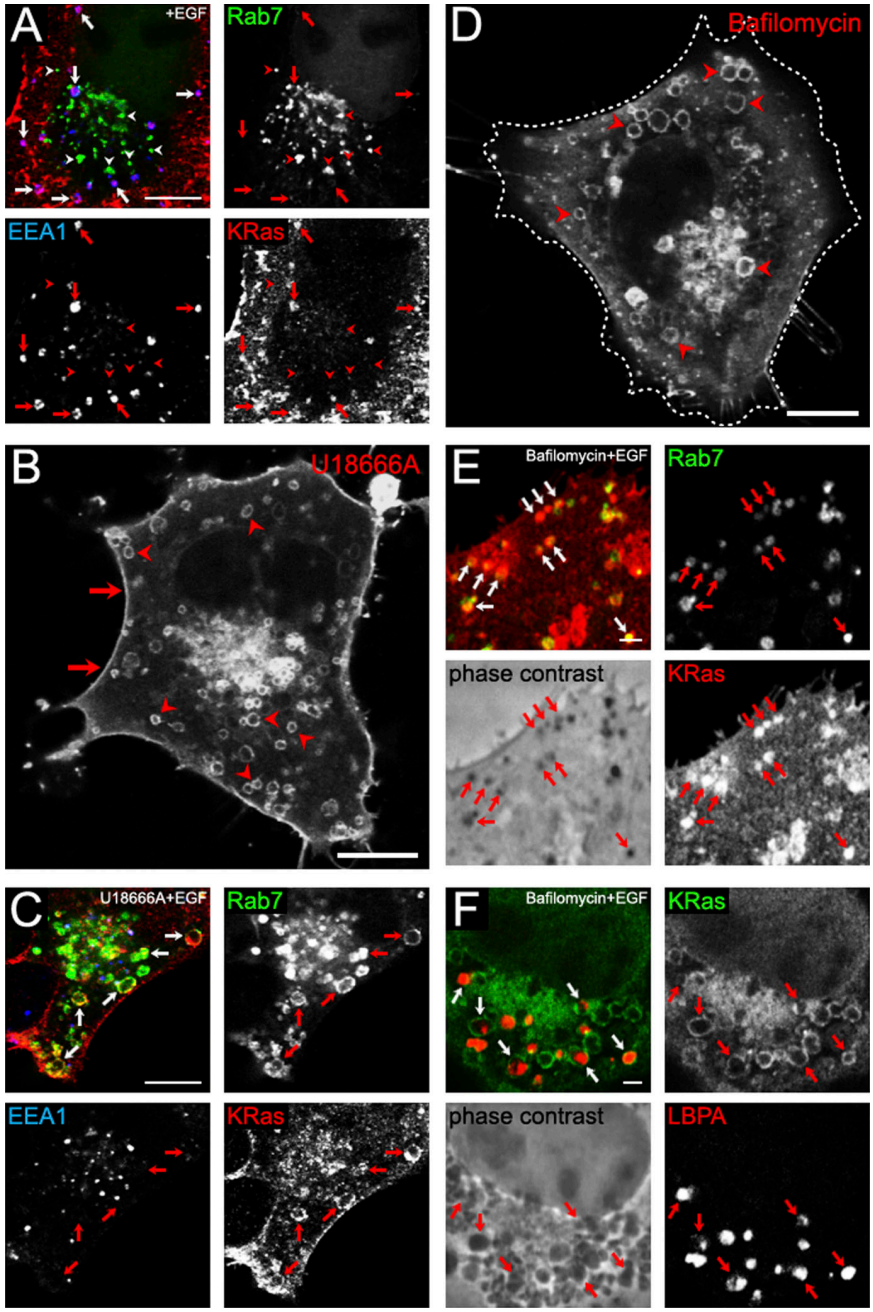

Figure 4. **U18666A and bafilomycin induce accumulation of KRas in a Rab7/LBPA late endosomal compartment.** (A) HA-KRas and GFP-Rab7–expressing cells were treated with EGF for 20 min and immunolabeled with an anti-HA (red channel) and anti-EEA1 (blue channel). Arrows indicate the colocalization of KRas and EEA1, and arrowheads point to Rab7-positive structures. (B) Localization of GFP-KRas in cells treated with U18666A. Arrows point to PM KRas labeling, and arrowheads show intracellular ringlike structures. (C) HA-KRas was coexpressed with GFP-Rab7 and treated with U18666A plus EGF for 45 min. Arrows show colocalization of HA-KRas with GFP-Rab7. (D–F) Localization of KRas in cells treated with 20 nM B-A1 overnight and with 100 ng/ml EGF for 45 min. Arrows indicate colocalization of HA-KRas and Rab7 (E) or GFP-KRas and LBPA (F) on enlarged endosomes. The white dotted contour in D indicates the cell perimeter, and the arrowheads point to ringlike endosomal structures. Bars: (A–D) 8 µm; (E and F) 2 µm.

drugs greatly enhanced accumulation of GFP-KRas and also the constitutively active mutant KRasG12V (not depicted) on enlarged endosomal structures (1–4 µm in diameter; Fig. 4, B and D). The B-A1–induced phenotype was also studied in living cells expressing GFP-KRas (Fig. S2 A). As KRas has also been found on mitochondria (Bivona et al., 2006; Plowman et al., 2008), we analyzed the possibility that the structures observed in B-A1–treated cells were mitochondria instead of endosomes. In vivo staining with the MitoTracker probe revealed that despite a slight mitochondrial staining of KRas (Fig. S2 B), the fluorescence observed on endosomal membranes was largely higher. Moreover, the presence of two MVB/late endosomal markers (GFP-Rab7 and endogenous lysobisphosphatidic acid [LBPA]) on these enlarged vesicles further confirmed the late endosomal nature of such structures (Fig. 4, C, E, and F). Finally, filipin staining confirmed the accumulation of cholesterol in KRas-positive LEs after U18666A treatment (Fig. S2 C).

Lysosomal targeting of KRas

Because KRas was detected on LEs, we aimed to study whether it may be targeted to the lysosomal compartment. In COS-1 cells, GFP-KRas colocalized to some extent with EGF-TRITC and the lysosomal marker LAMP1 (Fig. 5 A). We also analyzed KRas intracellular distribution in the presence of B-A1 or the lysosomal protease inhibitor leupeptin. In both cases, the intracellular colocalization of KRas with LAMP1 was significantly increased (Fig. 5, B–D). The same extent of colocalization was also obtained for LAMP2 (not depicted) or cathepsin D (see Fig. 8 D). The accumulation of KRas on the endolysosomal compartment was confirmed in different cell types treated with

B-A1 (Fig. S2, D–G). In contrast, GFP-HRas was found to be mainly present on Golgi membranes (Fig. 5, E and F). Similar data were obtained for GFP-NRas (Fig. S3, A and B).

High magnification confocal in vivo imaging enabled a more detailed analysis of the topology of KRas in those LEs. Interestingly, most of the GFP-KRas–expressing cells exhibited a variable number of MVB-like structures (in this study, we do not distinguish between different subpopulations of late endosomal compartments or MVBs) with a KRas staining on intralumenal membranes (Fig. 5 G). Tomographic sectioning allowed 3D reconstruction of such structures (Fig. 5 H and H′). Assuming that the thickness of the optical section is a function of the pinhole diameter, wavelength, refraction index, and numerical aperture for a 488-nm excitation wavelength, the optical section resolution thickness is ∼470–500 nm. Therefore, the size of the MVB-like structures analyzed was higher than 2–3 µm, and the mean intralumenal vesicle diameter was around 500 nm.

All of these results prompted us to study whether KRas targeted to this compartment could undergo lysosomal degradation. For this purpose, we monitored the stability of HA-tagged KRas in control or leupeptin plus B-A1–treated COS-1 cells after EGF stimulation under experimental conditions according to published data (Linares et al., 2007; Fasen et al., 2008; Hill et al., 2008). Results indicated that treated cells showed a significant increase in the stability of KRas as well as for the EGFR, which was used as a control (Fig. 5 J and Fig. S3 G). Similar results were obtained by [^{35}S]Met metabolic labeling experiments (Fig. S3, I–K); data analysis from these experiments shows that after EGF stimulation, the half-life of HA-KRas was 3.3 h, whereas in the absence of stimulation, it was 5.4 h. When cells were treated with lysosomal inhibitors, the half-life in both control and EGF-stimulated cells was 5.1 h and 6.6 h, respectively. In contrast, no changes were detected in KRas stability upon treatment with the proteasomal inhibitor MG132 (Fig. S3 H).

Finally, in an effort to detect the endogenous KRas on the endolysosomal compartment, GFP-Rab7–expressing COS-1 cells were treated with B-A1 and then subjected to immunocytochemical analysis using a pan-Ras antibody (because of the low labeling efficiency of the isoform-specific antibodies). Results revealed a considerable colocalization between Rab7 and endogenous Ras (Fig. 5 I). Under the same conditions but using nontransfected cells, we confirmed the presence of endogenous Ras on vesicles containing endocytosed EGF-TRITC or the endogenous lysosomal protease cathepsin D (Fig. S3, E and F). Thus, according to our results, we assume that the major isoform detected by this antibody in this compartment was the endogenous KRas. Therefore, we show for the first time that upon EGF stimulation, KRas is targeted to the lysosomal compartment, where it can be degraded.

Monitoring in vivo KRas activation on the endolysosomal system

We considered the possibility that the endolysosomal compartment acts as a new platform for KRas activation. Therefore, activation of KRas on LEs in B-A1–treated cells was measured by fluorescence recovery energy transfer (FRET) microscopy using the Raichu-KRas probe (Fig. S4 A; Kiyokawa et al., 2006). The probe was properly targeted to late endosomal membranes as seen in B-A1–treated cells cotransfected with RFP-Rab7 (Fig. S4 B). Also, upon EGF treatment, those LEs were labeled with the cotransfected EGFR–monomeric RFP (mRFP; Fig. S4 C). After 20–40 min of EGF stimulation, a high FRET efficiency of Raichu-KRas was observed on late endosomal membranes and also at the PM (Fig. 6 A and Videos 3 and 4). As a negative control, we used a Raichu-Pak-Rho probe (Yoshizaki et al., 2003), which did not show FRET efficiency on endosomal structures or at the PM (Fig. 6 B and Videos 5 and 6). Results were plotted according to the endosomal relative FRET ratio values measured from both Raichu probes only on endosomal membranes (Fig. 6 C). The FRET efficiency of Raichu-KRas reflects the activation state of the molecule, thus concluding that KRas can be activated on these Rab7-positive structures (Fig. S4 D). Importantly, under these conditions endosomal fusion was still functional. Indeed, we observed GFP-KRas–positive vesicles harboring internalized EGF-TRITC undergoing endosomal fusion (Fig. 6 D and Video 2).

Recruitment of Grb2 and Raf1 to KRas-positive LEs

It has been reported that Grb2 and Ras coordinately traffic during EGFR endocytosis (Jiang and Sorkin, 2002). Thus, we examined the recruitment of Grb2 to the endolysosomal compartment where KRas is present. Under B-A1 conditions, starved cells overexpressing Grb2-YFP showed a diffuse cytoplasmic distribution (Fig. 7 A). After 45 min of EGF-TRITC internalization, a high proportion of Grb2-YFP was efficiently redistributed together with the EGFR and its ligand to enlarged endocytic structures (Fig. 7 B). Nonstimulated cells cotransfected with CFP-KRas and Grb2-YFP only exhibited endosomal localization of KRas and EGFR (Fig. 7 C). However, EGF stimulation induced a clear recruitment of Grb2 to KRas-positive endosomes harboring both the EGFR and ligand (Fig. 7 D).

Finally, we investigated whether KRas present on the endolysosomal compartment was able to recruit Raf1. In nonstimulated cells coexpressing YFP-Raf1 and CFP-KRas, the distribution of Raf1 was mainly cytosolic, although some degree of colocalization with KRas-labeled vesicular structures could be identified (Fig. 7 G). Importantly, upon EGF-TRITC stimulation, a striking recruitment of Raf1 to late endosomal membranes positive for LAMP1 was observed (Fig. 7 H and Fig. S5 A). Under the same experimental conditions, when YFP-Raf1 was transfected alone, only a certain degree of colocalization of Raf1 with EGF-TRITC could be detected after 45 min of EGF endocytosis (Fig. 7, E and F). These results demonstrated that KRas, on this endolysosomal compartment, is susceptible to being activated and capable for signaling.

KRas-mediated MAPK signaling on LEs

To further link KRas localization on LEs to an established signaling pathway, we analyzed the possibility that KRas could be involved in the MAPK activation on LEs. It has been shown (Wunderlich et al., 2001) that p14, a protein specifically associated with the cytoplasmic leaflet of the LE, interacts with the scaffold protein MP1, which assembles a scaffold complex in

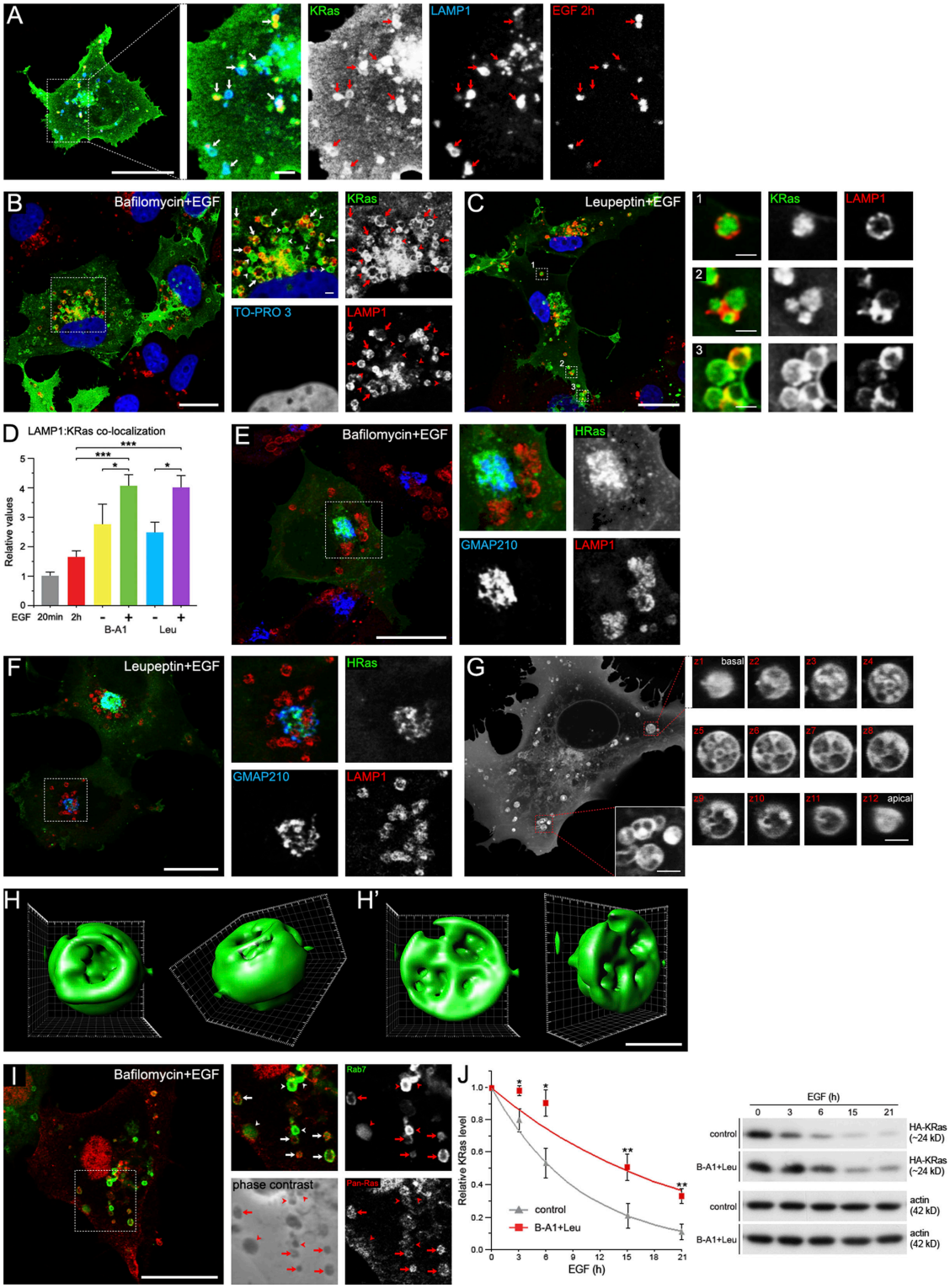

Figure 5. **Lysosomal targeting of KRas.** (A) COS-1 cells expressing GFP-KRas were treated with 100 ng/ml EGF-TRITC for 2 h. Triple labeling of GFP-KRas, LAMP1 (blue channel), and EGF-TRITC (red channel) is shown, and arrows indicate colocalization. (B and C) GFP-KRas–expressing cells were treated either with 20 nM B-A1 (B) or 25 µM leupeptin (C) and EGF. Immunolabeling with anti-LAMP1 antibody shows colocalization of KRas (green channel) with LAMP1 (red channel) on perinuclear ringlike structures (see arrows in insets of B and insets 1–3 of C); arrowheads (B, insets) point to KRas-positive vesicles not labeled with LAMP1. TO-PRO 3 is a nuclear marker (blue channel). (D) Quantification of LAMP1/GFP-KRas colocalization from experiments shown in A–C. Statistical significances of differences between different treatments were determined using the Student's *t* test. Data are means ± SEM; *, $P < 0.05$; ***, $P < 0.001$. (E and F) GFP-HRas–expressing cells treated with B-A1 (E) or leupeptin (F) and EGF show colocalization of HRas (green channel) with GMAP210 (Golgi marker; blue channel) but not with LAMP1 (red channel). (G) In vivo imaging of GFP-KRas–expressing cells after treatment with B-A1, leupeptin, and EGF reveals MVB-like structures containing intralumenal GFP-KRas–positive membranes (z1–z12). (H and H') 3D tomographic reconstruction of confocal sections z1–z11 (H) and z1–z7 (H'). (I) GFP-Rab7–expressing cells treated with B-A1 and EGF and labeled with anti–pan-Ras exhibit considerable colocalization (arrows). Arrowheads point to Rab7-positive vesicles not labeled with the pan-Ras antibody. (J) HA-KRas stability was measured in control

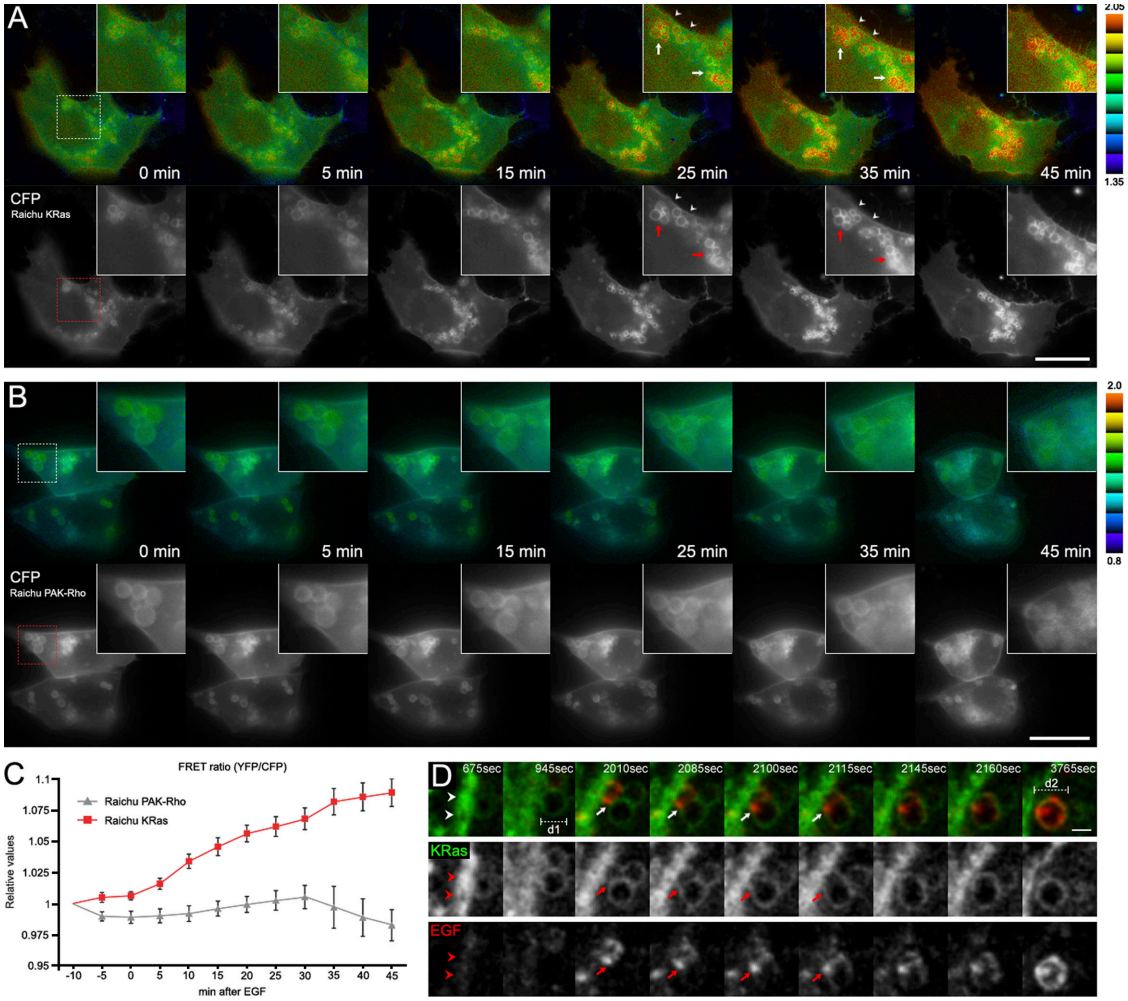

Figure 6. **Time-lapse recording of KRas activation on the late endosomal compartment.** (A and B) COS-1 cells were transfected with Raichu-KRas (A) or Raichu-Pak-Rho (B). Starved cells were treated with 20 nM B-A1 overnight and then with 100 ng/ml EGF for 50 min. In the top panels, representative ratio images of YFP/CFP at the indicated time points after EGF stimulation are shown. In the bottom panels, representative images of CFP–Raichu-KRas (A) and CFP–Raichu-Pak-Rho (B) indicate localization of the probes at each corresponding FRET image frame. All images in A and B were obtained every 5 min with a time-lapse epifluorescent microscope. High FRET efficiency can be observed at the PM (arrowheads) and on endosomal structures (arrows) between 25 and 45 min in Raichu-KRas–expressing cells only. (C) Quantification of FRET (FRET ratio of YFP/CFP) efficiency on the endocytic structures from at least six independent experiments was plotted for each time point by measuring the increase over the basal activity, which was averaged over 10 min before EGF addition. (D) Time-lapse video microscopy of COS-1 cells expressing GFP-KRas treated with B-A1 and with 100 ng/ml EGF-TRITC for 1.5 h. Confocal section images were collected every 15 s. Endosomal fusion of KRas-positive vesicles (green channel) harboring internalized EGF (red channel) is observed (arrows). Arrowheads point to PM-localized EGF-TRITC. Endosomal diameters d1 and d2 are 2.6 µm and 3.4 µm, respectively. Data are means ± SEM. Bars: (A and B) 20 µm; (D) 2 µm.

the extracellular signal-regulated kinase (ERK) cascade, eliciting a MAPK signal output from this intracellular compartment (Wunderlich et al., 2001; Teis et al., 2002, 2006). We found that after 45 min of EGF stimulation, Xpress-tagged p14 or myc-tagged MP1 colocalized with GFP-KRas (Fig. 8, A and C). This colocalization became more evident after B-A1 or leupeptin treatment on ringlike cathepsin D–positive structures (Fig. 8, B and D).

Next, we tried to study the kinetics of MAPK activation on the endolysosomal compartment by performing pulse-chase experiments with EGF. To determine the subcellular distribution of endogenous activated MAPK, we used an antibody that recognizes only the phosphorylated form of ERK1/2. Using confocal imaging, we analyzed the subcellular distribution of endogenous activated ERK1/2 in relation to the GFP-KRas/p14-positive endosomes after 5, 10, 30, or 60 min of EGF stimulation. Starved nonstimulated cells showed no significant phospho-ERK1/2 (pERK1/2) staining (Fig. 9 A). However, after 5 min of EGF stimulation, pERK1/2 staining could be detected

and B-A1 plus leupeptin–treated cells. Before stimulation with 100 ng/ml EGF, starved cells were preincubated for 6 h with 100 µg/ml CHX (control) or CHX in combination with B-A1 plus leupeptin (B-A1 + Leu). Equal amounts (15 µg) of cell lysates from 0, 3, 6, 15, and 21 h after EGF addition were electrophoresed, and the levels of HA-KRas detected with an anti-HA antibody in both control and B-A1 plus leupeptin–treated cells are shown (Western blot; $n = 5$). Actin was used as a loading control. Quantification analysis by densitometry was performed. Data are the mean ± SEM; *, $P < 0.05$; **, $P < 0.01$ (Student's t test). Bars: (A–C, E, F, and I), 20 µm; (G, H, and insets) 2 µm.

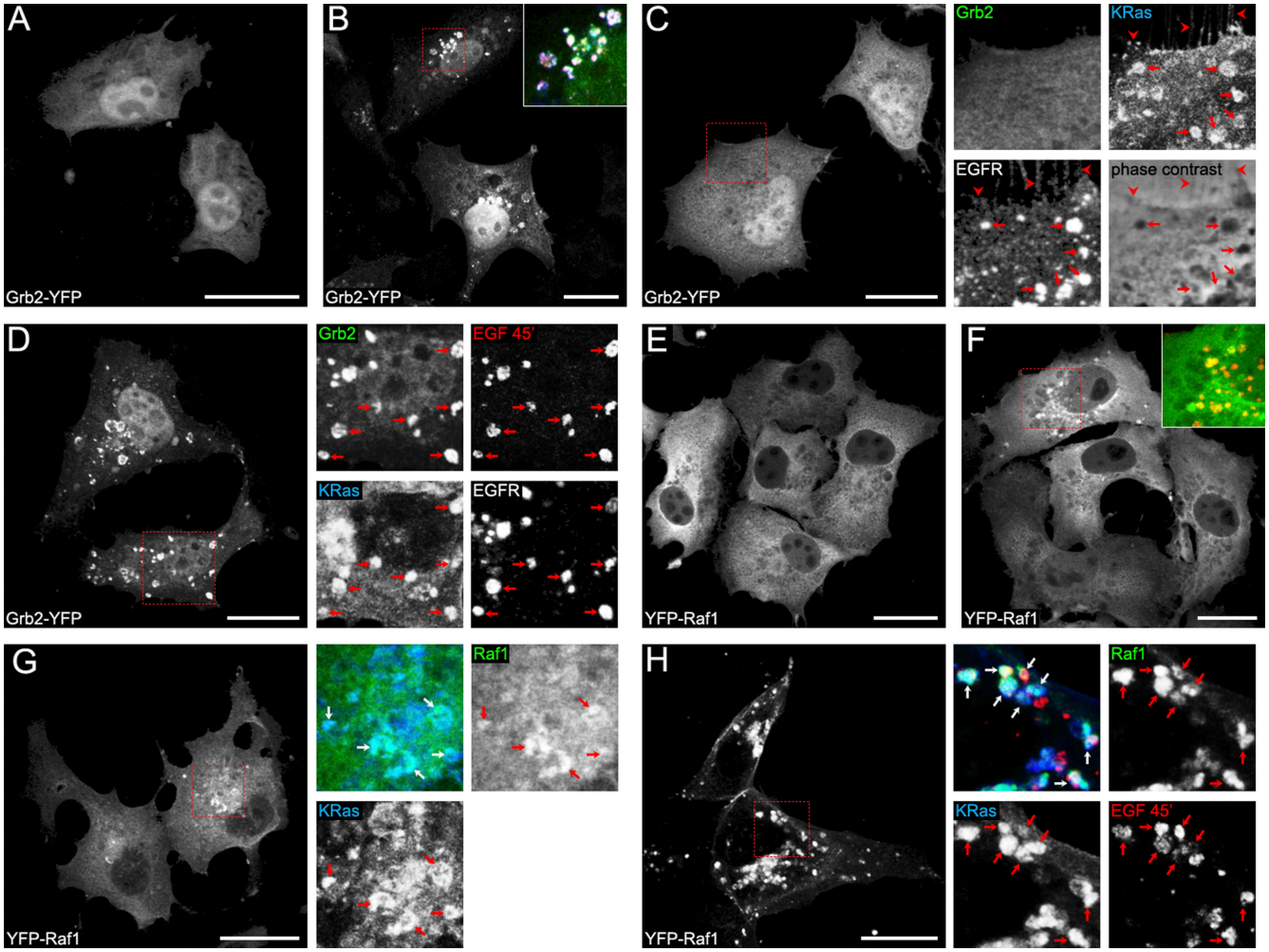

Figure 7. **Grb2 and Raf1 are recruited to KRas-positive LEs.** (A and B) COS-1 cells were transfected with Grb2-YFP and treated with B-A1 for 6 h. (A) Starved cells show diffuse cytosolic distribution of Grb2-YFP. (B) After 45 min of EGF-TRITC stimulation, Grb2 is redistributed onto perinuclear vesicles. Colocalization of EGF-TRITC (red channel), immunolabeled EGFR (blue channel), and Grb2 (green channel) is observed (inset). (C and D) Grb2-YFP and CFP-KRas were co-expressed in COS-1 cells, and then cells were treated with B-A1. (C) Control cells show diffuse cytoplasmic distribution of Grb2-YFP. Insets show colocalization of immunolabeled EGFR and CFP-KRas but not Grb2-YFP on both endosomes (arrows) and the PM (arrowheads). (D) After 45 min of EGF-TRITC stimulation, Grb2 is redistributed onto vesicular structures. Colocalization of EGF (red channel), immunolabeled EGFR (gray channel), Grb2 (green channel), and KRas (blue channel) is observed (arrows). (E and F) COS-1 cells were transfected with YFP-Raf1 and treated with B-A1 for 6 h. (E) Starved cells show diffuse cytoplasmic distribution of YFP-Raf1. (F) After 45 min of EGF-TRITC stimulation, Raf1 was recruited, to some extent, to vesicular structures (inset). Colocalization of internalized EGF (red channel) and Raf1 (green channel) could be observed (inset). (G and H) YFP-Raf1 and CFP-KRas were coexpressed in COS-1 cells, and then cells were treated with B-A1. (G) Control cells show a diffuse cytosolic pattern of YFP-Raf1. Some degree of colocalization of YFP-Raf1 (green channel) and CFP-KRas (blue channel) can be observed (white arrows in the merge inset and red arrows in the color channel insets). (H) After 45 min of EGF-TRITC stimulation, Raf1 is redistributed onto vesicular structures. Clear colocalization of endocytosed EGF (red channel), Raf1 (green channel), and KRas (blue channel) is observed (white arrows in the merge inset and red arrows in the color channel insets). (B–D and F–H) Dotted boxes define the areas from which the corresponding insets were generated. Bars, 20 µm.

at certain domains of the PM and some nuclei (Fig. 9 B). At this time point, no colocalization of pERK1/2 and KRas/p14-positive endosomes was observed. After 10 min of stimulation, the pERK1/2 signal was still observed at the PM, but partial staining could also be readily detected on GFP-KRas/p14-positive structures (Fig. 9 C). Such colocalization became more evident after 30 min of stimulation (Fig. 9 D). Even after the 60-min chase period, some cells still maintained the endosomal colocalization of pERK1/2, GFP-KRas, and p14 (Fig. 9 E).

We also performed biochemical analysis of ERK1/2 activation in control and leupeptin plus B-A1–treated COS-1 and NIH3T3-Wt8 cells expressing HA-KRas (Fig. 9, F and G). The relative activation of ERK1/2 was analyzed by densitometry (Fig. 9, F and G, graphs), revealing a sustained signaling in cells treated with the lysosomal inhibitors. However, in nontransfected cells, no significant sustained MAPK activation was observed (Fig. S5, B and C). Finally, we observed that the KRas-positive endosomal structures, in which endogenous pERK was detected, colocalized with endocytosed EGF-TRITC and the LysoTracker probe (Fig. 9, H and I). Thus, the major stability of KRas and the more sustained activation of ERK1/2 in cells treated with lysosomal inhibitors suggest that endosomal KRas-mediated MAPK signaling can be down-regulated in later stages of the endocytic pathway.

Discussion

The results presented in this study indicate that KRas translocates from the PM to the early and late endocytic compartment

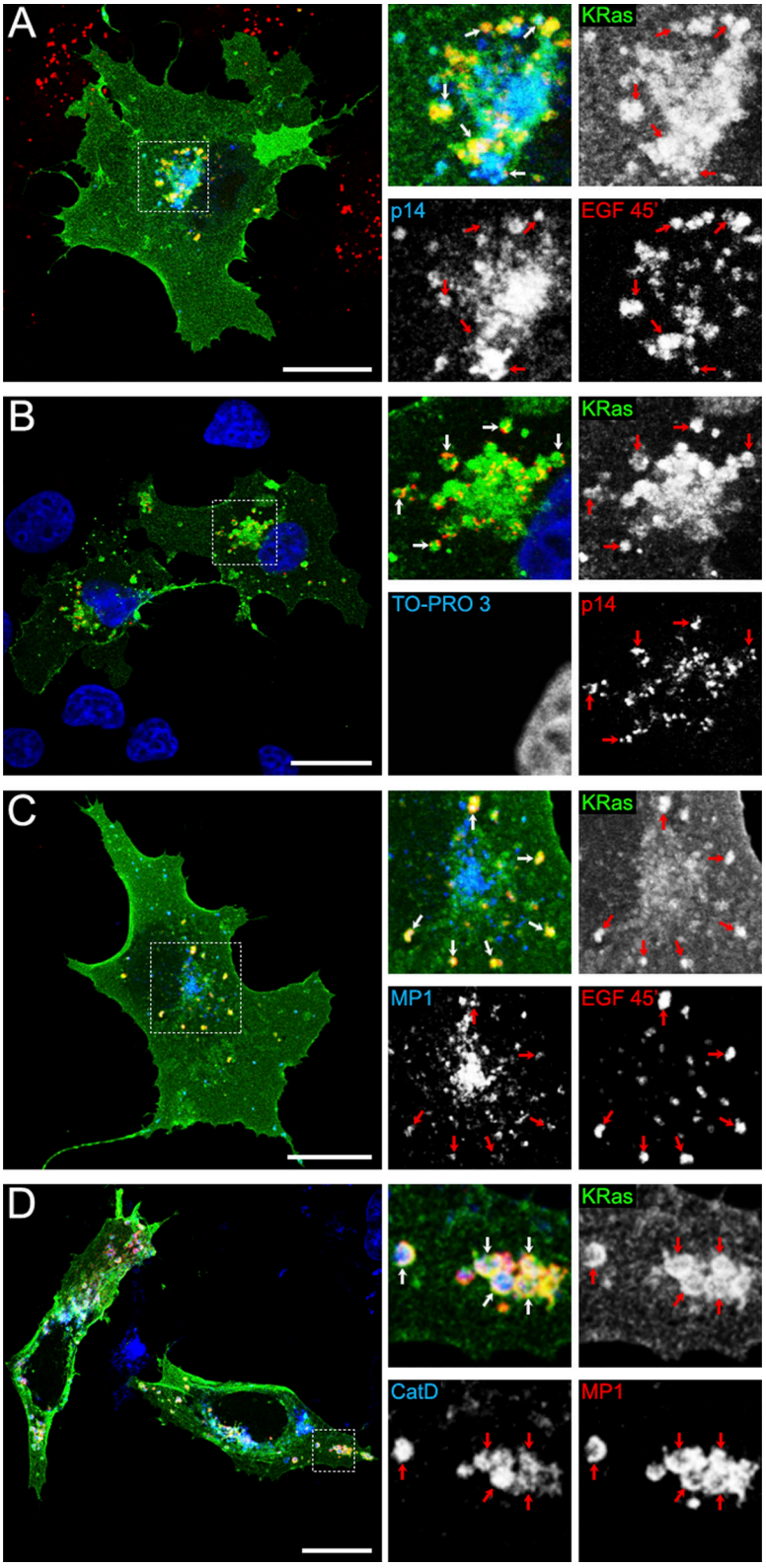

Figure 8. **KRas localizes on LEs containing the p14–MP1 scaffolding complex.** (A and B) COS-1 cells transiently co-expressing GFP-KRas and Xpress-tagged p14. (A) Colocalization of KRas (green channel) with p14 (blue channel) and endocytosed EGF-TRITC (100 ng/ml for 45 min) on perinuclear endosomes (insets). (B) Late endosomal colocalization of GFP-KRas and p14 after B-A1 treatment (20 nM for 6 h) in nonstimulated cells (insets). TO-PRO 3 is a nuclear marker (blue channel). (C and D) COS-1 cells were cotransfected with GFP-KRas and myc-tagged MP1. (C) Colocalization of KRas (green channel) with MP1 (blue channel) and endocytosed EGF-TRITC (red channel) on LEs (insets). (D) Triple labeling of GFP-KRas, MP1 (red channel), and cathepsin D (CatD; blue channel) is shown in cells treated with leupeptin for 8 h and EGF (100 ng/ml for 45 min; insets). Colocalization is indicated with white (merge) or red (separate channels) arrows. Dotted boxes define the areas from which the corresponding insets were generated. Bars, 20 μm.

through a clathrin-dependent pathway and independently of CaM and PKC phosphorylation. Then, from LEs, KRas is eventually targeted to lysosomes. FRET analysis using the Raichu-KRas probe shows that KRas is active on LEs and recruits Raf1 to elicit a MAPK signal output.

KRas is internalized via a clathrin-dependent pathway en route to the endocytic compartment

The localization of KRas on clathrin-coated pits and the abrogation of its internalization in cells expressing the dynamin

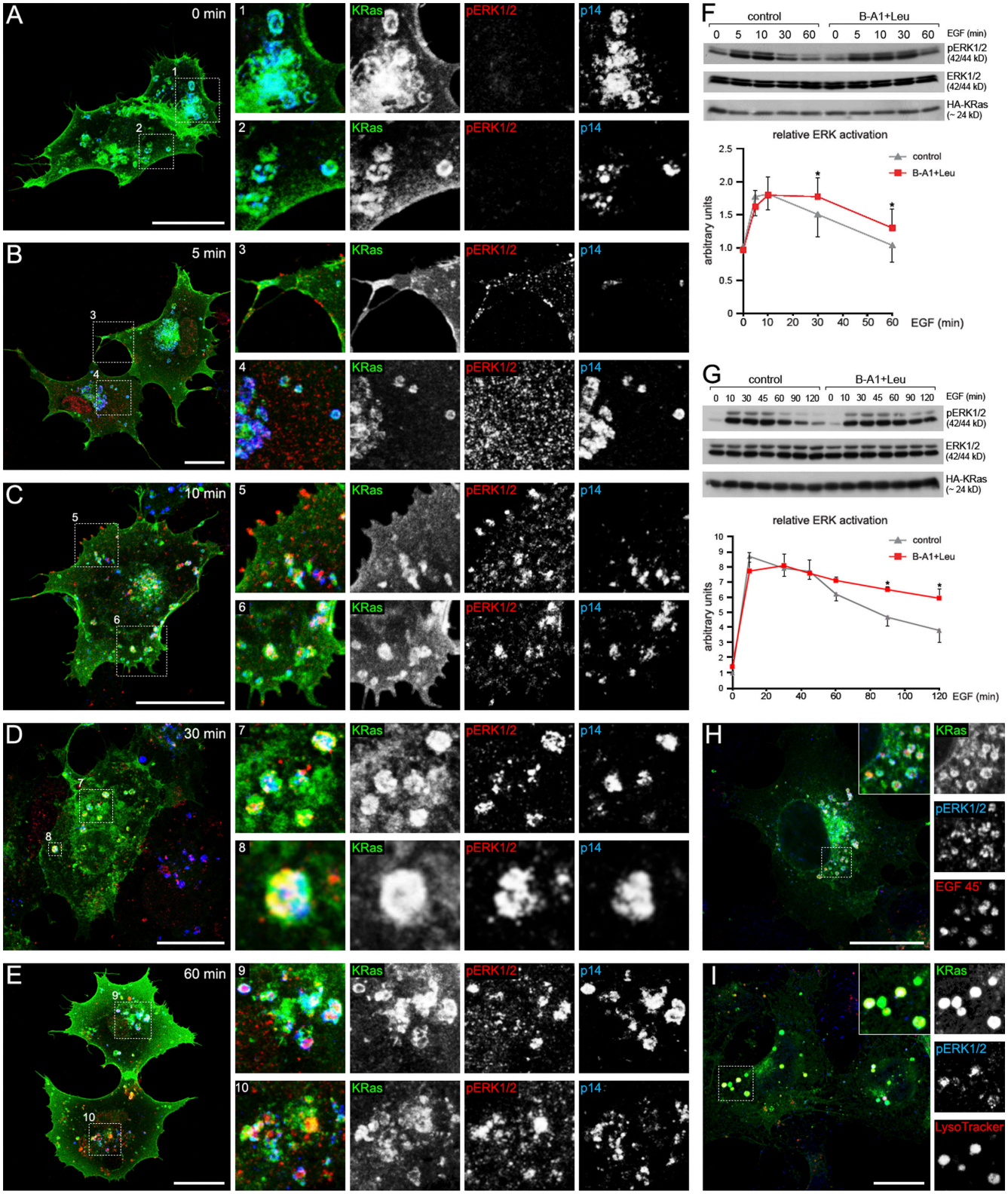

Figure 9. **KRas-mediated MAPK signaling on LEs.** (A–E) Cells coexpressing GFP-KRas with Xpress-tagged p14 were treated with 20 nM B-A1plus 25 µM leupeptin for 6 h and then were left starved or pulse-chase stimulated with 100 ng/ml EGF for various times before fixation. Cells were then subjected to indirect immunofluorescence analysis using anti-Xpress and anti-pERK1/2 antibodies. (A) The pERK1/2 antibody showed no staining in starved cells. KRas (green channel) colocalizes with p14 (blue channel)-positive endosomes (insets 1 and 2). (B) After 5 min of EGF stimulation, pERK1/2 labeling (red channel) can be readily detected on the PM (inset 3) and nuclei. Endosomal colocalization of KRas (green channel) and p14 (blue channel) is also shown (inset 4). (C–E) In cells that were stimulated with EGF for 10 (C), 30 (D), or 60 min (E), colocalization of pERK1/2 (red channel) with GFP-KRas and p14 (blue channel) was detected on endosomal structures (insets 5–10). After 10 min of EGF stimulation, pERK1/2 labeling can also be observed on the PM (inset 5). Insets 1–10 show magnifications of boxed areas. (F and G) COS-1 cells (F) and NIH3T3-Wt8 (G) cells were transiently transfected with HA-KRas

K44 mutant indicate that internalization of KRas takes place via a clathrin-dependent mechanism. It possibly occurs as a complex of signaling-related molecules in a similar mode as proposed by Jiang and Sorkin (2002), in which YFP-HRas and CFP-Grb2 together with the EGFR converge on endosomes. GFP-KRas was found on EEs in both resting and EGF-stimulated COS-1 (Fig. 1, A, B, and D–F), NIH3T3 (Fig. S1, A and B), or porcine aortic endothelial cells (not depicted), which is in agreement with previous studies (Jiang and Sorkin, 2002; Fivaz and Meyer, 2005; Gomez and Daniotti, 2007). On this compartment, GFP-KRas was found together with internalized EGF and its cognate receptor.

In this study, we report that a fraction of KRas is continuously endocytosed and sorted to LEs. Upon EGF stimulation, EGFR in complex with Grb2 is endocytosed and transported to LEs together with Grb2-binding proteins such as Sos, resulting in the activation of KRas on LEs. FRET detection kinetics of KRas activation on the late endosomal compartment is similar to that of the EGF-TRITC internalization.

Several studies indicated that KRas may be transported from the PM to intracellular compartments by diffusion mechanisms that rely on electrostatic gradients driving the polybasic domain within the KRas membrane anchor region (Fivaz and Meyer, 2005; Bivona et al., 2006; Gomez and Daniotti, 2007). This mechanism is similar to that described for myristoylated Ala-rich C kinase substrate, a protein that traffics from the PM to lysosomes (Allen and Aderem, 1995). In this study, we demonstrate for the first time in vivo endosomal fusion of GFP-KRas–labeled endosomes, providing new evidence that a KRas membrane–based trafficking also exists. Altogether, all of this evidence indicates that KRas translocation from the PM to endomembranes may proceed through different pathways, by diffusion or vesicular traffic (Fig. 10). The selection of one of these pathways probably depends on the cellular type but also on the specific stimuli and/or the intracellular destination (Ashery et al., 2006).

In this study, we show that enlarged LEs of cells treated with lysosomal perturbing agents allowed the identification of KRas on the perimeter membrane as well as on intralumenal membranes morphologically resembling MVB structures. These results are in agreement with previous data showing that taxol-treated cells redistribute GFP–truncated KRas (a GFP-tagged KRas-specific membrane anchor probe) to MVB-like structures (Apolloni et al., 2000). Moreover, a recent study demonstrates that proteins with cationic domains (like the KRas C-terminal polybasic motif) are preferentially recruited to phosphatidylserine-enriched organelles (such as endosomes or lysosomes; Yeung et al., 2008).

Importantly, although KRas accumulates on/in Rab7/LAMP1/cathepsin D/LysoTracker-positive structures, HRas and NRas remained excluded from this compartment, being mostly located on Golgi and the PM. Interestingly, a recent study showed that Ras levels are modulated after leupeptin treatment in an axin–β-catenin–overexpressing system, suggesting that lysosomal function may participate in the regulation of Ras protein levels (Jeon et al., 2007). In this study, we show that HA-KRas stability is significantly decreased when cells are stimulated with EGF. Interestingly, in EGF-stimulated cells exposed to lysosomal inhibitors, the half-life is increased. These results further support our model that EGF-induced trafficking of KRas leads to lysosomal degradation.

In vivo analysis of endosomal KRas signaling

Signaling at the late endocytic compartment has been demonstrated. The EGFR as well as other receptor Tyr kinases colocalize with signaling modules on endocytic compartments and can dictate different signal outputs from distinct subcellular locations (Jiang and Sorkin, 2002; Jiang et al., 2003; Huang et al., 2006; Hisata et al., 2007; Taub et al., 2007; Valdez et al., 2007). Scaffold and adapter proteins organize these signaling modules. Three scaffold proteins, the kinase suppressor of Ras-1 (KSR1), similar expression to *fgf* genes (Sef), and MP1, are known to assemble ERK complexes on different intracellular compartments. KSR1 regulates the formation of a MAPK signaling unit at the PM upon EGF stimulation (Mor and Philips, 2006). Sef selectively localizes MAPK/ERK kinase (MEK)–ERK complexes to the cytosolic face of the Golgi (Torii et al., 2004). Finally, the MP1 scaffold forms a stable heterodimeric complex with the adapter protein p14 and assembles an ERK cascade on the LE (Wunderlich et al., 2001). Endosomal localization of the p14–MP1 complex is required for the activation of ERK on these structures (Lunin et al., 2004). However, Jiang and Sorkin (2002) showed FRET between CFP-HRas and YFP–Ras-binding domain on endosomal membranes in vivo. Altogether, these studies support the idea that traffic from the PM to the LE is connected with signaling events in the cell.

In this study, we report the targeting of KRas to late endosomal membranes, where it colocalizes with the p14–MP1 scaffolding complex and activates the ERK signaling cascade. In addition, by means of the Raichu-KRas probe, we report activation of KRas on LEs. Because the membrane-anchoring motifs of the intramolecular FRET probes in this study consist of the native KRas polybasic sequence and CAAX moiety, it is likely that these domains represent the minimal membrane-interacting requirement that targets KRas to late endosomal membranes.

The recruitment of Raf1 by KRas on LEs indicates that in this compartment, KRas actively mediates intracellular signal

and serum starved for 20 h. Control cells or cells treated with the lysosomal inhibitors B-A1 plus leupeptin (B-A1 + Leu) were then stimulated with EGF by pulse and chase for the indicated times. Cell lysates were separated by SDS-PAGE and probed with the indicated antibodies (Western blot; $n = 5$). The graphs show a densitometric analysis of ERK1/2 relative activation. The pERK1/2 signals were normalized against the ERK1/2 signals. Data are the mean ± SEM; *, $P < 0.05$ (Student's *t* test). (H) B-A1–treated cells expressing GFP-KRas were stimulated with 100 ng/ml EGF-TRITC for 45 min before fixation. Colocalization of KRas (green channel) with immunolabeled pERK1/2 (blue channel) and EGF (red channel) is observed on ringlike structures (insets). (I) Leupeptin-treated cells expressing GFP-KRas were loaded with LysoTracker red DND-99 and incubated in the presence of 100 ng/ml EGF at 37°C for 45 min before fixation. Colocalization of KRas (green channel) with immunolabeled pERK1/2 (blue channel) and LysoTracker (red channel) is observed on ringlike structures (insets). (H and I) Dotted boxes define the areas from which the corresponding insets were generated. Bars, 20 µm.

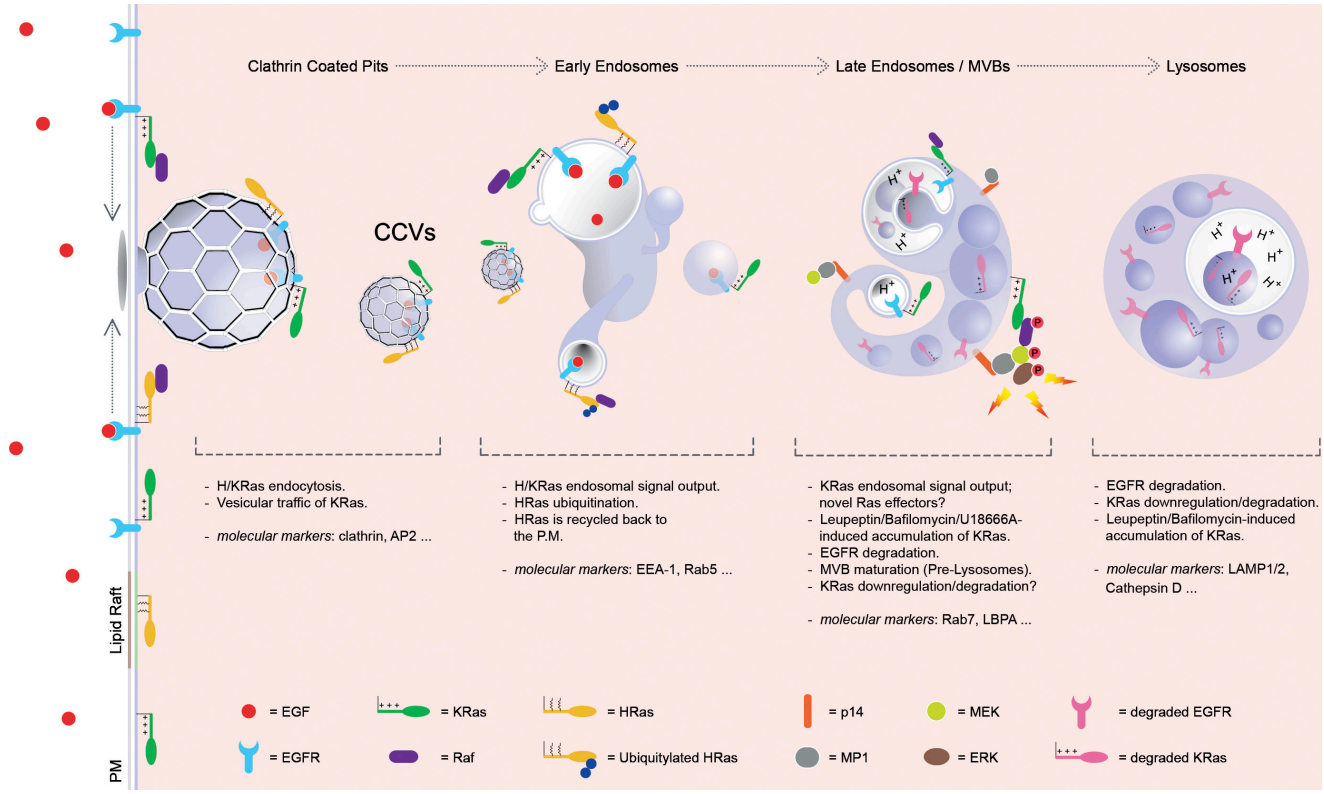

Figure 10. **Model of the endosomal KRas traffic and signaling.** EGF binding triggers endocytosis of the EGFR and downstream signaling molecules to the early endosomal compartment. There, Ras signaling modules settle to elicit signal outputs. HRas is ubiquitinated and is recycled back to the PM, whereas KRas is sorted en route to LEs/MVBs. Once there, KRas can be GTP loaded, thus being able to recruit effectors such as Raf1, which initiates the MAPK signaling cascade on this compartment. Finally, KRas down-regulation/degradation may occur in the late endosomal/lysosomal compartment. CCV, clathrin-coated vesicle.

outputs through specific effectors. Interestingly, Corey and Kelley (2007) recently reported an elevated Ras activity in Niemann-Pick disease type C cells. Because Niemann-Pick disease type C cells contain aberrant LEs with morphological features similar to those shown in this study, we speculate that such Ras activation could be explained by an increased KRas accumulation/activity on this aberrant late endosomal compartment.

Whereas a previous study (Roy et al., 2002) showed that endocytosis was not necessary for KRas signaling, in this study, we demonstrate that in addition to a PM signal output, the LE can be envisaged as a novel KRas signaling platform. However, further studies will be required to evidence the physiological role of KRas signaling on LEs as well as the cross talk between other signaling molecules (i.e., p14 and MP1) on this compartment.

Overall, this study sheds new light on the spatiotemporal control of Ras signaling, providing new clues on the distinctive behavior of Ras proteins in the cell and how endosomal traffic orchestrates this behavior. Thus, we propose the LE as a novel KRas signaling platform. From this compartment, KRas triggers functional outputs while en route to lysosomes, where signaling will be attenuated/down-regulated.

Materials and methods

Plasmids

HRas, KRas, and Raf1 cDNAs were provided by R. Marais (Institute of Cancer Research, London, England, UK) and subcloned into living color vectors (Clontech Laboratories, Inc.). The GFP-NRas vector was supplied by J. Miyazaki (Osaka University, Osaka, Japan; Niwa et al., 1991). The HA-HRas vector (pCEFLHA) was provided by P. Crespo (Consejo Superior de Investigaciones Científicas, Santander, Spain). Plasmids for mRFP-Rab7 and EGFR-mRFP have been described previously (Itoh et al., 2005; Kawase et al., 2006). The EGFR-CFP, Grb2-YFP, and pEGFP-Rab7 vectors were supplied by A. Sorkin (University of Colorado, Denver, Denver, CO). The pEF–HA-KRas plasmid was obtained from R. Marais. KRas (Ser181A) and KRas (Ser181D) mutants were obtained by PCR with reverse or forward oligonucleotides carrying the appropriate mutations. The Raichu-KRas and Raichu-Pak-Rho probes used in this study have been developed previously (Mochizuki et al., 2001; Yoshizaki et al., 2003). The Xpress-p14 and myc-MP1 constructs were a gift from L.A. Huber (Innsbruck Medical University, Innsbruck, Austria).

Antibodies and reagents

Mouse EGF, W13, U18666A, B-A1, and leupeptin were obtained from Sigma-Aldrich; BIM-I and anti–pan-Ras (ab-3; Ras10) antibody were obtained from EMD. EGF-TRITC, rhodamine-transferrin, and the MitoTracker red and LysoTracker DND-99 probes were obtained from Invitrogen. Mouse monoclonal anti-EGFR (clone 225) and anti–clathrin heavy chain (×22) antibodies were obtained from A. Sorkin and F.M. Brodsky (University of California, San Francisco, San Francisco, CA), respectively. The GMAP210 polyclonal antibody was supplied by R.M. Rios (Universidad de Sevilla, Sevilla, Spain). Monoclonal antibodies to EEA1 and LAMP1 were obtained from Transduction Laboratories. The monoclonal antiactin antibody was obtained from ICN Pharmaceuticals, and the polyclonal antibodies against EGFR (clone 1,005), KRas (F234), Rab5, and cathepsin D were obtained from Santa Cruz Biotechnology, Inc. The pERK1/2 and ERK1/2 antibodies were purchased from Cell Signaling Technology. Monoclonal anti-GFP antibody was obtained from Assay Designs. Polyclonal and monoclonal anti-HA antibodies were obtained from Sigma-Aldrich and Roche, respectively. Peroxidase-labeled antibodies and SDS-PAGE molecular weight markers were purchased from Bio-Rad Laboratories. Monoclonal anti-Xpress antibody was obtained

from Invitrogen, and monoclonal anti–myc tag clone 9E10 was purchased from Millipore.

Cell culture and transfections

COS-1, HeLa, and VERO cells were grown in DME (Biological Industries) containing 10% FBS (Biological Industries), pyruvic acid, antibiotics, and Gln. Porcine aortic endothelial cells were grown in Ham's F12 (Biological Industries) containing 10% FBS, pyruvic acid, antibiotics, and Gln. NIH3T3 cells (clone Wt8) stably expressing 4 × 105 human EGFRs/cell were provided by A. Sorkin. Transient expressions were performed using Effectene (QIAGEN) according to the manufacturer's specifications. Cells were used 12–36 h after transfection and starved at least 12 h before each experiment.

Immunofluorescence and quantitative image analysis

Cells grown on coverslips were fixed with 4% paraformaldehyde, permeabilized with 0.1% Triton X-100, and blocked with 1% BSA in PBS for 15 min at 37°C. Cells were incubated with the indicated primary antibodies and subsequently with secondary antibodies labeled with Alexa Fluor 488, 594, and 647 (Invitrogen) or Cy5 (Jackson ImmunoResearch Laboratories); finally, coverslips were mounted with Mowiol (EMD). The immunofluorescence protocol for endogenous pERK1/2 detection has been previously described (Teis et al., 2002). Confocal images were acquired using a laser-scanning confocal spectral microscope (TCS SL; Leica) with argon and HeNe lasers attached to an inverted microscope (DMIRE2; Leica). Colocalization of GFP-KRas with EEA1 on endosomal structures was quantified using ImageJ software (National Institutes of Health) and the Colocalization Highlighter plugin (P. Bourdoncle, Institute Jacques Monod, Service Imagerie, Paris, France). The Colocalization Highlighter plugin generated an image of colocalized pixels (binary). Then, with the ImageJ process Image Calculator plugin (minimum operation), the values of the colocalized points were converted to the real value of green (green colocalization image). After this, all images were converted into 32 bits, and original thresholds were set with the background as NaN (not a number). Finally, a total cell region of interest was defined, and the integrated density of both the green colocalization image and the 32-bit threshold green image was measured for the specified area. The ratio of these two resulting values was defined as the percentage of green colocalization. Results were normalized to the control condition, and statistical analysis was conducted by a Student's *t* test.

Imaging of KRas activity in living cells

COS-1 cells were plated on 35-mm glass-base dishes (Asahi Techno Glass Co.) and then transfected with plasmid Raichu–derived vectors (Raichu-KRas and Raichu-Pak-Rho). Starved cells were treated with 20 nM B-A1 overnight and then with 100 ng/ml EGF for 50 min. Images were obtained every 5 min, starting 10 min before and ending 50 min after EGF addition, on an inverted epifluorescent microscope (IX81; Olympus) that was equipped with a cooled charge-coupled device camera (CoolSNAP HQ; Roper Scientific) and controlled by MetaMorph software (MDS Analytical Technologies). For dual-emission ratio imaging of Raichu probes, we used a 440AF21 excitation filter, a 455DRLP dichroic mirror, and two emission filters, 480AF30 for CFP and 535AF26 for YFP (all from Omega Optical, Inc.), as described previously (Mochizuki et al., 2001). Cells were illuminated with a 75-W xenon lamp through a 12% neutral density filter (Olympus) and a 100× oil immersion objective lens. The exposure time was 400 ms when the binning of the charge-coupled device camera was set to 4 × 4 binning. After background subtraction, the ratio image of YFP/CFP was created with MetaMorph software and used to represent the FRET efficiency. The relative FRET values from specified regions of interest corresponding to vesicular structures were averaged for each time point and then plotted on a graph. In the cotransfection experiments, mRFP-Rab7 or EGFR-mRFP was introduced along with plasmid Raichu–KRas. A dichroic mirror (86006bs; Chroma Technology Corp.) was used when RFP fluorescence was monitored with FRET probes. An XF1207 (580AF20) excitation filter and an XF3015 (636DF55) emission filter were used for RFP imaging. After background subtraction, FRET/CFP ratio images were created using MetaMorph software, and the images were used to represent FRET efficiency.

Quantification of the KRas stability using lysosomal inhibitors

Starved COS-1 cells transfected with HA-KRas were pooled and then plated in 60-mm dishes at 80% confluence. Then, an equal number of dishes were preincubated for 6 h either with 100 µg/ml cycloheximide (CHX; Sigma-Aldrich) alone or in combination with the lysosomal inhibitors leupeptin (15 µM) and B-A1 (20 nM). Immediately after this, a 0-h time point lysate was obtained, and 100 ng/ml EGF was added in all of the remaining dishes. At 3, 6, 15, and 21 h after EGF, additional medium was removed, and cells were washed twice with cold PBS and then frozen at −80°C. Cells were lysed with lysis buffer (20 mM Tris-HCl, pH 7.5, 2 mM EDTA, 100 mM NaCl, 5 mM $MgCl_2$, 1% Triton X-100, 5 mM NaF, 10% glycerol, and 0.5% 2-mercaptoethanol) containing protease and phosphatase inhibitors. Cleared lysates (10,000 *g*) were assayed for protein concentration, and 15 µg of protein was subjected to Western blot analysis using specific HA and actin antibodies. HA-KRas signal was determined by densitometry and normalized to the actin levels. Data were analyzed by a Student's *t* test. Alternatively, in some experiments, metabolic labeling using [^{35}S]Met was performed.

Phospho-MAPK analysis

Pulse and chase experiments were performed using starved COS-1 cells nontransfected or transfected with HA-KRas. After 15 h of transfection, cells were stimulated by pulse chase with 100 ng/ml EGF at 37°C for the indicated times. Then, medium was removed, and cells were washed twice with cold PBS and frozen at −80°C. Cells were lysed with lysis buffer (see previous section) containing protease and phosphatase inhibitors. Cleared lysates (10,000 *g*) were assayed for protein concentration, and 15 µg of protein was subjected to Western blot analysis using anti-MEK1/2, anti–phospho-MEK1/2, anti-ERK1/2, and anti-pERK1/2 antibodies. The phospho-MEK1/2 and pERK1/2 signals were normalized against the MEK1/2 and ERK1/2 signals, respectively. Data were analyzed by a Student's *t* test.

Online supplemental material

Fig. S1 shows early endosomal localization of KRas. Fig. S2 shows that the LE to lysosome transition inhibitors induce accumulation of KRas in the late endosomal compartment. Fig. S3 provides further data on the lysosomal targeting and degradation of KRas. Fig. S4 depicts a schematic representation of the Raichu-KRas probe and shows in vivo localization of this probe in B-A1–treated cells together with data on the activation dynamics of KRas on LEs. Fig. S5 demonstrates that KRas recruits Raf1 to late endosomal membranes and also shows further data on the effect of lysosomal inhibitors on MAPK signaling. Video 1 shows in vivo visualization of endosomal GFP-KRas after EGF stimulation. Video 2 shows live imaging of endosomal fusion of GFP-KRas–positive endosomes. Videos 3 and 4 show FRET imaging of Raichu-KRas on LEs. Videos 5 and 6 show FRET imaging of Raichu-Pak-Rho on LEs. Online supplemental material is available at http://www.jcb.org/cgi/content/full/jcb.200807186/DC1.

We thank Dr. A. Sorkin for critical comments on the manuscript and for supplying vectors. We are very grateful to Dr. L.A. Huber for revision of the manuscript and for supplying important constructs used in this study. We would also like to thank Drs. M. Kitano and K. Aoki for valuable comments on the paper and discussions.

This study was supported by grants from Ministerio de Educación y Ciencia of Spain (BFU2006-01151/BMC and V-2006-RET2008-0 to C. Enrich, SAF2006-5212 and SAF2003-08339 to O. Bachs, SAF2007-60491 to N. Agell, and BFU2007-67652 to F. Tebar). A. Lu is thankful to Ministerio de Educación y Ciencia of Spain (Formación Profesorado Universitario mobility program) for a short-term fellowship at the laboratory of M. Matsuda.

Submitted: 30 July 2008
Accepted: 17 February 2009

References

Allen, L.A., and A. Aderem. 1995. Protein kinase C regulates MARCKS cycling between the plasma membrane and lysosomes in fibroblasts. *EMBO J.* 14:1109–1121.

Apolloni, A., I.A. Prior, M. Lindsay, R.G. Parton, and J.F. Hancock. 2000. H-ras but not K-ras traffics to the plasma membrane through the exocytic pathway. *Mol. Cell. Biol.* 20:2475–2487.

Ashery, U., O. Yizhar, B. Rotblat, and Y. Kloog. 2006. Nonconventional trafficking of Ras associated with Ras signal organization. *Traffic*. 7:119–126.

Bivona, T.G., I. Perez De Castro, I.M. Ahearn, T.M. Grana, V.K. Chiu, P.J. Lockyer, P.J. Cullen, A. Pellicer, A.D. Cox, and M.R. Philips. 2003. Phospholipase Cgamma activates Ras on the Golgi apparatus by means of RasGRP1. *Nature*. 424:694–698.

Bivona, T.G., S.E. Quatela, B.O. Bodemann, I.M. Ahearn, M.J. Soskis, A. Mor, J. Miura, H.H. Wiener, L. Wright, S.G. Saba, et al. 2006. PKC regulates a

farnesyl-electrostatic switch on K-Ras that promotes its association with Bcl-XL on mitochondria and induces apoptosis. *Mol. Cell*. 21:481–493.

Caloca, M.J., J.L. Zugaza, and X.R. Bustelo. 2003. Exchange factors of the RasGRP family mediate Ras activation in the Golgi. *J. Biol. Chem.* 278:33465–33473.

Chiu, V.K., T. Bivona, A. Hach, J.B. Sajous, J. Silletti, H. Wiener, R.L. Johnson II, A.D. Cox, and M.R. Philips. 2002. Ras signalling on the endoplasmic reticulum and the Golgi. *Nat. Cell Biol.* 4:343–350.

Corey, D.A., and T.J. Kelley. 2007. Elevated small GTPase activation influences the cell proliferation signaling control in Niemann-Pick type C fibroblasts. *Biochim. Biophys. Acta*. 1772:748–754.

Damke, H., T. Baba, D.E. Warnock, and S.L. Schmid. 1994. Induction of mutant dynamin specifically blocks endocytic coated vesicle formation. *J. Cell Biol.* 127:915–934.

de Diego, I., F. Schwartz, H. Siegfried, P. Dauterstedt, J. Heeren, U. Beisiegel, C. Enrich, and T. Grewal. 2002. Cholesterol modulates the membrane binding and intracellular distribution of annexin 6. *J. Biol. Chem.* 277:32187–32194.

Fasen, K., D.P. Cerretti, and U. Huynh-Do. 2008. Ligand binding induces Cbl-dependent EphB1 receptor degradation through the lysosomal pathway. *Traffic*. 9:251–266.

Fivaz, M., and T. Meyer. 2005. Reversible intracellular translocation of KRas but not HRas in hippocampal neurons regulated by Ca^{2+}/calmodulin. *J. Cell Biol.* 170:429–441.

Gomez, G.A., and J.L. Daniotti. 2005. H-Ras dynamically interacts with recycling endosomes in CHO-K1 cells: involvement of Rab5 and Rab11 in the trafficking of H-Ras to this pericentriolar endocytic compartment. *J. Biol. Chem.* 280:34997–35010.

Gomez, G.A., and J.L. Daniotti. 2007. Electrical properties of plasma membrane modulate subcellular distribution of K-Ras. *FEBS J.* 274:2210–2228.

Grewal, T., J. Heeren, D. Mewawala, T. Schnitgerhans, D. Wendt, G. Salomon, C. Enrich, U. Beisiegel, and S. Jackle. 2000. Annexin VI stimulates endocytosis and is involved in the trafficking of low density lipoprotein to the prelysosomal compartment. *J. Biol. Chem.* 275:33806–33813.

Hancock, J.F. 2003. Ras proteins: different signals from different locations. *Nat. Rev. Mol. Cell Biol.* 4:373–384.

Hill, M.M., M. Bastiani, R. Luetterforst, M. Kirkham, A. Kirkham, S.J. Nixon, P. Walser, D. Abankwa, V.M. Oorschot, S. Martin, et al. 2008. PTRF-Cavin, a conserved cytoplasmic protein required for caveola formation and function. *Cell*. 132:113–124.

Hisata, S., T. Sakisaka, T. Baba, T. Yamada, K. Aoki, M. Matsuda, and Y. Takai. 2007. Rap1-PDZ-GEF1 interacts with a neurotrophin receptor at late endosomes, leading to sustained activation of Rap1 and ERK and neurite outgrowth. *J. Cell Biol.* 178:843–860.

Howe, C.L., J.S. Valletta, A.S. Rusnak, and W.C. Mobley. 2001. NGF signaling from clathrin-coated vesicles: evidence that signaling endosomes serve as a platform for the Ras-MAPK pathway. *Neuron*. 32:801–814.

Huang, F., D. Kirkpatrick, X. Jiang, S. Gygi, and A. Sorkin. 2006. Differential regulation of EGF receptor internalization and degradation by multiubiquitination within the kinase domain. *Mol. Cell*. 21:737–748.

Itoh, R.E., K. Kurokawa, A. Fujioka, A. Sharma, B.J. Mayer, and M. Matsuda. 2005. A FRET-based probe for epidermal growth factor receptor bound non-covalently to a pair of synthetic amphipathic helixes. *Exp. Cell Res.* 307:142–152.

Jeon, S.H., J.Y. Yoon, Y.N. Park, W.J. Jeong, S. Kim, E.H. Jho, Y.J. Surh, and K.Y. Choi. 2007. Axin inhibits extracellular signal-regulated kinase pathway by Ras degradation via beta-catenin. *J. Biol. Chem.* 282:14482–14492.

Jiang, X., and A. Sorkin. 2002. Coordinated traffic of Grb2 and Ras during epidermal growth factor receptor endocytosis visualized in living cells. *Mol. Biol. Cell*. 13:1522–1535.

Jiang, X., F. Huang, A. Marusyk, and A. Sorkin. 2003. Grb2 regulates internalization of EGF receptors through clathrin-coated pits. *Mol. Biol. Cell*. 14:858–870.

Jura, N., E. Scotto-Lavino, A. Sobczyk, and D. Bar-Sagi. 2006. Differential modification of Ras proteins by ubiquitination. *Mol. Cell*. 21:679–687.

Kawase, K., T. Nakamura, A. Takaya, K. Aoki, K. Namikawa, H. Kiyama, S. Inagaki, H. Takemoto, A.R. Saltiel, and M. Matsuda. 2006. GTP hydrolysis by the Rho family GTPase TC10 promotes exocytic vesicle fusion. *Dev. Cell*. 11:411–421.

Kiyokawa, E., S. Hara, T. Nakamura, and M. Matsuda. 2006. Fluorescence (Forster) resonance energy transfer imaging of oncogene activity in living cells. *Cancer Sci.* 97:8–15.

Linares, L.K., R. Kiernan, R. Triboulet, C. Chable-Bessia, D. Latreille, O. Cuvier, M. Lacroix, L. Le Cam, O. Coux, and M. Benkirane. 2007. Intrinsic ubiquitination activity of PCAF controls the stability of the oncoprotein Hdm2. *Nat. Cell Biol.* 9:331–338.

Liscum, L., and J.R. Faust. 1989. The intracellular transport of low density lipoprotein-derived cholesterol is inhibited in Chinese hamster ovary cells cultured with 3-beta-[2-(diethylamino)ethoxy]androst-5-en-17-one. *J. Biol. Chem.* 264:11796–11806.

Lopez-Alcala, C., B. Alvarez-Moya, P. Villalonga, M. Calvo, O. Bachs, and N. Agell. 2008. Identification of essential interacting elements in K-Ras/calmodulin binding and its role in K-Ras localization. *J. Biol. Chem.* 283:10621–10631.

Lunin, V.V., C. Munger, J. Wagner, Z. Ye, M. Cygler, and M. Sacher. 2004. The structure of the MAPK scaffold, MP1, bound to its partner, p14. A complex with a critical role in endosomal map kinase signaling. *J. Biol. Chem.* 279:23422–23430.

Malumbres, M., and M. Barbacid. 2003. RAS oncogenes: the first 30 years. *Nat. Rev. Cancer*. 3:459–465.

Mochizuki, N., S. Yamashita, K. Kurokawa, Y. Ohba, T. Nagai, A. Miyawaki, and M. Matsuda. 2001. Spatio-temporal images of growth-factor-induced activation of Ras and Rap1. *Nature*. 411:1065–1068.

Mor, A., and M.R. Philips. 2006. Compartmentalized Ras/MAPK signaling. *Annu. Rev. Immunol.* 24:771–800.

Niwa, H., K. Yamamura, and J. Miyazaki. 1991. Efficient selection for high-expression transfectants with a novel eukaryotic vector. *Gene*. 108:193–199.

Oh, P., D.P. McIntosh, and J.E. Schnitzer. 1998. Dynamin at the neck of caveolae mediates their budding to form transport vesicles by GTP-driven fission from the plasma membrane of endothelium. *J. Cell Biol.* 141:101–114.

Perez de Castro, I., T.G. Bivona, M.R. Philips, and A. Pellicer. 2004. Ras activation in Jurkat T cells following low-grade stimulation of the T-cell receptor is specific to N-Ras and occurs only on the Golgi apparatus. *Mol. Cell. Biol.* 24:3485–3496.

Plowman, S.J., N. Ariotti, A. Goodall, R.G. Parton, and J.F. Hancock. 2008. Electrostatic interactions positively regulate K-Ras nanocluster formation and function. *Mol. Cell. Biol.* 28:4377–4385.

Pol, A., M. Calvo, and C. Enrich. 1998. Isolated endosomes from quiescent rat liver contain the signal transduction machinery. Differential distribution of activated Raf-1 and Mek in the endocytic compartment. *FEBS Lett.* 441:34–38.

Prior, I.A., A. Harding, J. Yan, J. Sluimer, R.G. Parton, and J.F. Hancock. 2001. GTP-dependent segregation of H-ras from lipid rafts is required for biological activity. *Nat. Cell Biol.* 3:368–375.

Quatela, S.E., and M.R. Philips. 2006. Ras signaling on the Golgi. *Curr. Opin. Cell Biol.* 18:162–167.

Recchi, C., and P. Chavrier. 2006. V-ATPase: a potential pH sensor. *Nat. Cell Biol.* 8:107–109.

Roy, S., R. Luetterforst, A. Harding, A. Apolloni, M. Etheridge, E. Stang, B. Rolls, J.F. Hancock, and R.G. Parton. 1999. Dominant-negative caveolin inhibits H-Ras function by disrupting cholesterol-rich plasma membrane domains. *Nat. Cell Biol.* 1:98–105.

Roy, S., B. Wyse, and J.F. Hancock. 2002. H-Ras signaling and K-Ras signaling are differentially dependent on endocytosis. *Mol. Cell. Biol.* 22:5128–5140.

Tall, G.G., M.A. Barbieri, P.D. Stahl, and B.F. Horazdovsky. 2001. Ras-activated endocytosis is mediated by the Rab5 guanine nucleotide exchange activity of RIN1. *Dev. Cell*. 1:73–82.

Taub, N., D. Teis, H.L. Ebner, M.W. Hess, and L.A. Huber. 2007. Late endosomal traffic of the epidermal growth factor receptor ensures spatial and temporal fidelity of mitogen-activated protein kinase signaling. *Mol. Biol. Cell*. 18:4698–4710.

Teis, D., W. Wunderlich, and L.A. Huber. 2002. Localization of the MP1-MAPK scaffold complex to endosomes is mediated by p14 and required for signal transduction. *Dev. Cell*. 3:803–814.

Teis, D., N. Taub, R. Kurzbauer, D. Hilber, M.E. de Araujo, M. Erlacher, M. Offterdinger, A. Villunger, S. Geley, G. Bohn, et al. 2006. p14-MP1-MEK1 signaling regulates endosomal traffic and cellular proliferation during tissue homeostasis. *J. Cell Biol.* 175:861–868.

Tian, T., A. Harding, K. Inder, S. Plowman, R.G. Parton, and J.F. Hancock. 2007. Plasma membrane nanoswitches generate high-fidelity Ras signal transduction. *Nat. Cell Biol.* 9:905–914.

Torii, S., M. Kusakabe, T. Yamamoto, M. Maekawa, and E. Nishida. 2004. Sef is a spatial regulator for Ras/MAP kinase signaling. *Dev. Cell*. 7:33–44.

Valdez, G., P. Philippidou, J. Rosenbaum, W. Akmentin, Y. Shao, and S. Halegoua. 2007. Trk-signaling endosomes are generated by Rac-dependent macroendocytosis. *Proc. Natl. Acad. Sci. USA*. 104:12270–12275.

van Weert, A.W., K.W. Dunn, H.J. Gueze, F.R. Maxfield, and W. Stoorvogel. 1995. Transport from late endosomes to lysosomes, but not sorting of integral membrane proteins in endosomes, depends on the vacuolar proton pump. *J. Cell Biol.* 130:821–834.

Villalonga, P., C. Lopez-Alcala, M. Bosch, A. Chiloeches, N. Rocamora, J. Gil, R. Marais, C.J. Marshall, O. Bachs, and N. Agell. 2001. Calmodulin binds to K-Ras, but not to H- or N-Ras, and modulates its downstream signaling. *Mol. Cell. Biol.* 21:7345–7354.

Wunderlich, W., I. Fialka, D. Teis, A. Alpi, A. Pfeifer, R.G. Parton, F. Lottspeich, and L.A. Huber. 2001. A novel 14-kilodalton protein interacts with the mitogen-activated protein kinase scaffold mp1 on a late endosomal/lysosomal compartment. *J. Cell Biol.* 152:765–776.

Yeung, T., G.E. Gilbert, J. Shi, J. Silvius, A. Kapus, and S. Grinstein. 2008. Membrane phosphatidylserine regulates surface charge and protein localization. *Science*. 319:210–213.

Yoshizaki, H., Y. Ohba, K. Kurokawa, R.E. Itoh, T. Nakamura, N. Mochizuki, K. Nagashima, and M. Matsuda. 2003. Activity of Rho-family GTPases during cell division as visualized with FRET-based probes. *J. Cell Biol.* 162:223–232.